

Expected Improvement Matrix-based Infill Criteria for Expensive Multiobjective Optimization

Dawei Zhan, Yuansheng Cheng, and Jun Liu

Abstract—The existing multiobjective expected improvement criteria are often computationally expensive because they are calculated using multivariate piecewise integrations, the number of which increases exponentially with the number of objectives. In order to solve this problem, this work proposes a new approach to develop cheap-to-evaluate multiobjective expected improvement criteria based on the proposed expected improvement matrix. The elements in the expected improvement matrix are the single-objective expected improvements that the studying point has beyond each Pareto front approximation point in each objective. Three multiobjective criteria are developed by combining the elements in the expected improvement matrix into scalar functions in three different ways. These proposed multiobjective criteria are calculated using only one-dimensional integrations, whose number increases linearly with respect to the number of objectives. Moreover, all the three criteria are derived in closed form expressions, thus are significantly cheaper to evaluate than the state-of-the-art multiobjective criteria. The efficiencies of the proposed criteria are validated through 12 test problems. Besides the computational advantage, the proposed multiobjective expected improvement criteria also show competitive abilities in approximating the Pareto fronts of the chosen test problems compared against the state-of-the-art multiobjective expected improvement criteria.

Index Terms—Efficient global optimization, expected improvement, expensive multiobjective optimization, Kriging model.

I. INTRODUCTION

MANY practical optimization problems have multiple objectives and the evaluations of these objectives are often computationally expensive. These optimization problems are defined as expensive multiobjective optimization problems and allow only a limited number of evaluations. Multiobjective evolutionary algorithms, such as NSGA-II algorithm [1], often need thousands (or tens of thousands) of function evaluations to provide a suitable Pareto front approximation, which might not be acceptable for computationally expensive objectives.

Surrogate model-based optimization method is one way to solve the expensive optimization problems [2]–[4]. In the optimization process, the computationally expensive models are replaced by some previously built surrogate models, so that the evaluations of the time-consuming models can be minimized. The efficient global optimization (EGO) algorithm [5]–[7] is one of the most widely used surrogate model-based optimization methods in expensive single-objective optimization. The EGO algorithm starts by building a Kriging model, also known as the Gaussian process model, using a small set of

D. Zhan, Y. Cheng and J. Liu are with the School of Naval Architecture and Ocean Engineering, Huazhong University of Science and Technology, Wuhan, 430074 China (email: zhandawei@hust.edu.cn; yscheng@hust.edu.cn; hustlj@hust.edu.cn).

evaluated solutions. In each cycle, an infill sampling criterion named expected improvement (EI) is maximized to select the next candidate to evaluate. The process iterates in this way until some stopping condition is met. The EI criterion was first defined by Mockus *et al.* [8], [9] and popularized by Schonlau [5] and Jones *et al.* [6]. It is derived in closed form expression, thus is cheap to calculate. More importantly, it gives an elegant balance between local exploitation and global exploration when deciding which point to evaluate. The EI criterion has been improved [10], [11] and extended to constrained problems [12], [13] and noisy problems [14]–[16]. Besides being used in the EGO algorithms as an infill criterion, the EI criterion is also used in evolutionary algorithm (EA) as a prescreening criterion [17], [18].

When dealing with expensive multiobjective problems, studies have been carried out to generalize the single-objective EGO algorithm to multiobjective optimization in the last ten years. Different ideas have been proposed. Shinkyu *et al.* [19] used a multiobjective optimization method to optimize the EI of all objectives, and considered the obtained Pareto solutions as promising candidates. Knowles [20] and Zhang *et al.* [21] extended the single-objective EGO algorithm into multiobjective EGO algorithms by scaling the objectives into one weighted sum function. The weights in their algorithms [20], [21] are changed throughout the optimization process. Wagner *et al.* [22] worked on a multiobjective infill criterion which measures the increment of the hypervolume when the lower confidence bound of a point is added to the Pareto front approximation. A penalty is used in this criterion to consider the prediction uncertainty and to support a good distribution of the Pareto front approximation. There are also approaches that directly extend the single-objective EI to multiobjective EI by integrating a defined multiobjective improvement function over the non-dominated area. The expected hypervolume improvement (EHVI) criterion was first defined by Emmerich in his Ph.D. thesis [17] and was used as a prescreening criterion in multiobjective evolutionary algorithms at that time. Then Łaniewski-Wołk *et al.* [23] used the EHVI as an infill criterion and Shimoyama *et al.* [24] further studied it by comparing it to other multiobjective infill criteria. Keane [25] and Bautista [26] used the Euclidean distance and maximin distance as the multiobjective improvements and proposed the Euclidean distance-based and maximin distance-based EI criteria respectively for the multiobjective EGO algorithm.

Directly generalizing the single-objective EI criterion to multiobjective EI criterion is intuitive and appealing. The benefits of directly deriving multiobjective EI criteria are three fold. First, the simple and classic framework of the

single-objective EGO algorithm can be kept. Second, the multiobjective EI criterion can inherit the theoretic characters of the single-objective EI criterion, such as the convergence property and the balance property between local exploitation and global exploration. Third, a large number of improvements and extensions of the classic EI criterion can be directly used on the multiobjective EI criterion, such as extensions of dealing with constrained problems and noisy problems.

There are some differences between the single-objective and multiobjective EI criteria. The ‘current best solution’ in single-objective problem would become the ‘current non-dominated front’ in multiobjective problem. The improvement function is simply the one-dimensional distance between the studying point and the ‘current best solution’ in single-objective case, and should be redefined in the multi-dimensional objective space. The univariate integration would become multivariate integration when calculating the expected value of the improvement, and the integration region would change from a one-dimensional line to an irregular area (or volume, even hypervolume). Last but not the least, the target of multiobjective EI algorithms would be finding the best approximated Pareto optimal solutions instead of a single optimal solution in single-objective EI algorithms.

Current studies about multiobjective EI criteria have the same routine. First, define a kind of improvement function upon the current Pareto front approximation. Then calculate the expected value of the improvement function by integrating the improvement function over the non-dominated region. Due to the complexity of the non-dominated region, the integral region is often decomposed into a sum of h (h scales exponentially with the number of objectives) regular cells, and piecewise integration is used to calculate the expected improvement value. When the number of objectives is higher than two, the piecewise integration becomes so tedious that the closed form formulas of these multiobjective EI criteria are hard to provide, which makes the computations of these multiobjective EI criteria typically time-consuming. The existing multiobjective EI criteria differ in the defined improvement functions. The three most studied multiobjective improvement functions are the Euclidean distance improvement [25], [27], the maximin distance improvement [26], [28], [29], and the hypervolume improvement [17], [18], [23]. Although works have been done to reduce the computational time of these multiobjective EI criteria [30], [31], there is still no computationally cheap algorithm when the number of objective is higher than two. The heavy computational burden of these multiobjective EI criteria becomes a barrier preventing their usages in practical problems.

This work proposes a new approach to develop three cheap-to-evaluate and still efficient multiobjective EI criteria. The new approach, based on the concept of the proposed expected improvement matrix (EIM), tries to use a combination of $k \times m$ (k is the number of current non-dominated front points and m is the number of objectives) simple one-dimensional integrations to calculate the multiobjective expected improvement. Neither piecewise integration nor Monte Carlo integration is needed. The new proposed EIM criteria are provided in closed forms and are very cheap to evaluate no matter how many

objectives and non-dominated front points the problem has. The monotonicity properties of the newly proposed multiobjective EI criteria are studied. Numerical experiments are conducted to study their efficiencies compared to the state-of-the-art multiobjective EI criteria.

II. THE SINGLE-OBJECTIVE EI CRITERION

A. The Kriging model

Given N n -dimensional points $\mathbf{x}^1, \mathbf{x}^2, \dots, \mathbf{x}^N \in R^n$ and their associated responses f^1, f^2, \dots, f^N , the Kriging model, or the Gaussian process model, is built as

$$y(\mathbf{x}) = \mu + \varepsilon(\mathbf{x}), \quad (1)$$

where μ and $\varepsilon(\mathbf{x})$ are the mean and error term of the Gaussian process respectively. μ is a constant for a simple Kriging model, and $\varepsilon(\mathbf{x})$ is normally distributed with mean zero and variance σ^2 . Usually a spatial correlation between the error terms of two points \mathbf{x}^i and \mathbf{x}^j is assumed. The common-used correlation functions are the squared exponential function, the Matérn function and the exponential function [32]. In the field of design and analysis of computer experiments (DACE), the squared exponential function with additional hyperparameters is often used

$$\text{Corr}\left[\varepsilon(\mathbf{x}^i), \varepsilon(\mathbf{x}^j)\right] = \exp\left(-\sum_{k=1}^n \theta_k |x_k^i - x_k^j|^{p_k}\right), \quad (2)$$

where $\theta_k > 0$ and $p_k \in \{1, 2\}$. As a result, the Kriging model is determined by $2n+2$ parameters: $\mu, \sigma^2, \theta_1, \dots, \theta_n, p_1, \dots, p_n$. These parameters are tuned by maximizing the likelihood of the observed points. The detailed derivation can be found in [33]. Then the Kriging model offers the prediction of the unvisited point \mathbf{x}

$$\hat{y}(\mathbf{x}) = \hat{\mu} + \mathbf{l}^T \mathbf{C}^{-1} (\mathbf{y} - \mathbf{1}\hat{\mu}), \quad (3)$$

and its associated mean squared error

$$s^2(\mathbf{x}) = \hat{\sigma}^2 \left[1 - \mathbf{c}^T \mathbf{C}^{-1} \mathbf{c} + \frac{(1 - \mathbf{1}^T \mathbf{C}^{-1} \mathbf{c})^2}{\mathbf{1}^T \mathbf{C}^{-1} \mathbf{1}} \right], \quad (4)$$

where \mathbf{C} is a matrix with entry $C_{ij} = \text{Corr}[\varepsilon(\mathbf{x}^i), \varepsilon(\mathbf{x}^j)]$, \mathbf{c} is an N -dimensional vector with entry $c_i = \text{Corr}[\varepsilon(\mathbf{x}), \varepsilon(\mathbf{x}^i)]$, $\mathbf{y} = (f^1, f^2, \dots, f^N)$ is the vector of the N observed function value, and $\mathbf{1}$ is N -dimensional vector of ones.

B. The Expected Improvement Criterion

The response of the studying point \mathbf{x} is normally distributed

$$Y(\mathbf{x}) \sim N(\hat{y}(\mathbf{x}), s^2(\mathbf{x})), \quad (5)$$

and the improvement of the studying point beyond the current best solution is defined [6] as

$$I(\mathbf{x}) = \max(f_{\min} - Y(\mathbf{x}), 0), \quad (6)$$

where f_{\min} is the current best observation. The expected improvement criterion is the expected value of the improvement $I(\mathbf{x})$ [6], that is

$$EI(\mathbf{x}) =$$

$$(f_{\min} - \hat{y}(\mathbf{x})) \Phi\left(\frac{f_{\min} - \hat{y}(\mathbf{x})}{s(\mathbf{x})}\right) + s(\mathbf{x}) \phi\left(\frac{f_{\min} - \hat{y}(\mathbf{x})}{s(\mathbf{x})}\right), \quad (7)$$

where $s(\mathbf{x})$ is the square root of the Kriging prediction variance; $\Phi(\mathbf{x})$ and $\phi(\mathbf{x})$ are the Gaussian cumulative distribution function and probability density function respectively.

III. REVIEW OF MULTIOBJECTIVE EI CRITERIA

A. Expensive Multiobjective Optimization Problem

This paper considers the following continuous multiobjective optimization problem with only box constraints:

$$\begin{aligned} \text{find } \mathbf{x} &= (x_1, x_2, \dots, x_n) \\ \text{minimize } F(\mathbf{x}) &= \{f_1(\mathbf{x}), f_2(\mathbf{x}), \dots, f_m(\mathbf{x})\} \\ \text{subject to } x_i &\in [a_i, b_i] \quad i = 1, 2, \dots, n \end{aligned} \quad (8)$$

where a_i and b_i are real constants, and $a_i < b_i$ for all $i = 1, 2, \dots, n$. The dimension of the search (design) space is n and the dimension of the objective space is m . In this work, the objectives are assumed to be noise-free and expensive to evaluate.

Assume that N initial points are generated and evaluated on the expensive objectives. The current Pareto front approximation can be identified among the N initial design points using non-dominated sorting method

$$PF_{approx} = \{f_1^j, f_2^j, \dots, f_m^j\} \quad j = 1, 2, \dots, k, \quad (9)$$

where k is the number of current non-dominated points and $k \leq N$. Each objective is approximated by a Kriging model. The objective vector of the studying point \mathbf{x} then can be considered as the following m -dimensional Gaussian random variables:

$$Y_i(\mathbf{x}) \sim N(\hat{y}_i(\mathbf{x}), s_i^2(\mathbf{x})) \quad i = 1, 2, \dots, m, \quad (10)$$

where $\hat{y}_i(\mathbf{x})$ and $s_i^2(\mathbf{x})$ are the prediction and variance value of the studying point \mathbf{x} offered by the i th Kriging model. The multi-dimensional Gaussian models are usually assumed to be mutually independent, because they are easier to implement. Besides, it has been shown that using dependent Gaussian models gains little, sometime no benefits compared against the independent Gaussian models [29]. Therefore, the independent Gaussian models are used in this paper.

The probability density function and the cumulative distribution function of the m -dimensional independent Gaussian random variables can be expressed respectively as

$$g(y_1, y_2, \dots, y_m) = \prod_{i=1}^m \frac{1}{s_i} \phi\left(\frac{y_i - \hat{y}_i}{s_i}\right) \quad (11)$$

and

$$G(y_1, y_2, \dots, y_m) = \prod_{i=1}^m \Phi\left(\frac{y_i - \hat{y}_i}{s_i}\right). \quad (12)$$

A two-dimensional example is shown in Fig. 1. It can be seen that the objective space is divided into two parts by the non-dominated front: the dominated area and the non-dominated area. The dark point and the cloud around the point show the probability density function of the objective vector of the studying point.

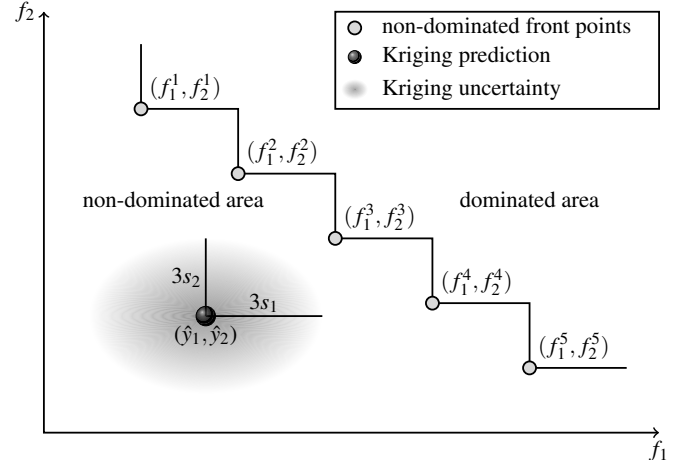


Fig. 1. A two-dimensional example of the non-dominated front.

B. State-of-the-art Multiobjective EI Criteria

The state-of-the-art multiobjective improvement functions are Euclidean distance improvement [25], maximin distance improvement [29] and hypervolume improvement [17], [18], respectively. The Euclidean distance improvement is defined by Keane [25] as the Euclidean distance between the objective vector of \mathbf{x} to its nearest non-dominated front point

$$I_e(\mathbf{x}) = \min_{j=1}^k \sqrt{\sum_{i=1}^m (f_i^j - y_i(\mathbf{x}))^2}. \quad (13)$$

The maximin distance-based multiobjective EI criterion is first introduced by Bautista [26] and then modified by Svenson *et al.* [28], [29]. The idea of maximin distance came from the maximin fitness function in a multiobjective evolutionary algorithm [34]. The (modified) maximin distance function measures the axis-wise distance between the objective vector of \mathbf{x} and the Pareto front approximation

$$I_m(\mathbf{x}) = -\max_{j=1}^k \left[\min_{i=1}^m (y_i(\mathbf{x}) - f_i^j) \right]. \quad (14)$$

The hypervolume indicator [35] measures the volume (or hypervolume) of the region dominated by the Pareto front approximation S , bounded by a reference point

$$H(S) = \text{Volume}\{\mathbf{y} \in R^m \mid S \prec \mathbf{y} \prec \mathbf{r}\}, \quad (15)$$

where the reference point \mathbf{r} is chosen by the user and should be dominated by all the points in the Pareto front approximation. The illustration of a two-dimensional hypervolume is given in Fig. 2. The hypervolume indicator [36] is often used to assess the quality of a Pareto approximation set and is reported to be the only scalar indicator that is strictly monotonic with regard to Pareto dominance. The hypervolume indicator is used increasingly in multiobjective evolutionary algorithms [37]–[39]. The principal problem with hypervolume indicator is that it is expensive to compute when the number of objectives is higher than two. However, the appealing mathematical properties of the hypervolume indicator has drawn lots of research to develop different algorithms for faster calculation of the hypervolume indicator [40]–[43].

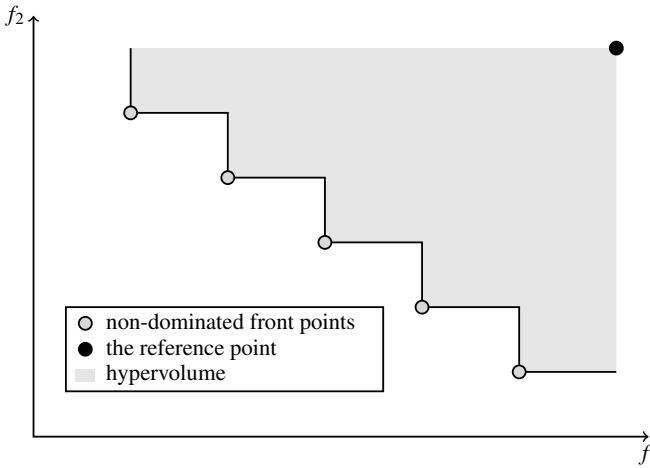


Fig. 2. A two-dimensional example of the hypervolume indicator.

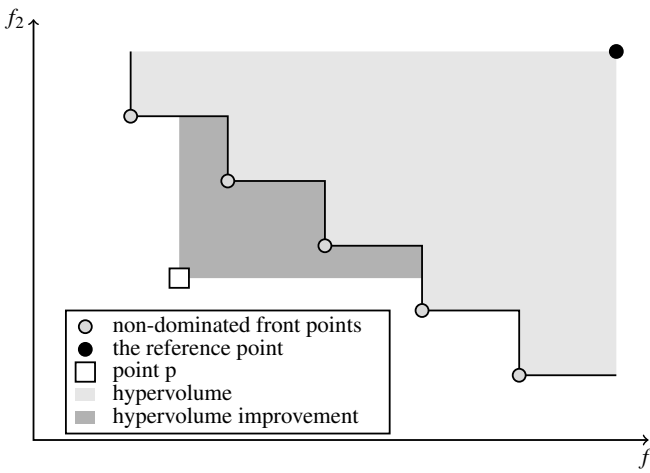


Fig. 3. A two-dimensional example of the hypervolume improvement.

The hypervolume improvement, which is illustrated in Fig. 3, is the improvement in hypervolume when a point p is added to the Pareto front approximation S

$$I_h(\mathbf{x}) = H(S \cup p) - H(S). \quad (16)$$

The multiobjective expected improvement is calculated by integrating the defined multiobjective improvement function over the whole non-dominated region A , that is

$$EI(\mathbf{x}) = \int_{y \in A} I(\mathbf{x}) \prod_{i=1}^m \frac{1}{s_i} \phi\left(\frac{y_i - \hat{y}_i}{s_i}\right) dy_i. \quad (17)$$

Replace the $I(\mathbf{x})$ in the above equation with $I_e(\mathbf{x})$, $I_m(\mathbf{x})$ and $I_h(\mathbf{x})$, then one can get the $EI_e(\mathbf{x})$, $EI_m(\mathbf{x})$ and $EI_h(\mathbf{x})$ respectively.

Directly integrating the Euclidean distance improvement in (13) over the non-dominated area gives no closed form expression, even for the 2-objective instance. For simplification, Keane [25] calculated the centroid of the improvement distribution and applied the Euclidean distance between the

centroid point and its nearest Pareto point as the expected improvement

$$EI_e(\mathbf{x}) = PI(\mathbf{x}) \min_{j=1}^k \sqrt{\sum_{i=1}^m (y_i^* - f_i^j)^2}, \quad (18)$$

where $PI(\mathbf{x})$ is the multiobjective probability of improvement, y_i^* is the centroid of the improvement distribution in i th direction. Keane [25] provided the closed form formula for 2-objective problems through piecewise integration and pointed out that the formulas for problems with more than two objective functions remain in closed form. However, the number of cells for piecewise integration increases exponentially with the number of objectives. Therefore, it is hard to give the specific expressions when the number of objectives is higher than two. In practice, Monte Carlo integration is less accurate but much simpler and faster to implement for higher number of objectives. Recently, Couckuyt *et al.* [30] proposed a fast algorithm for the exact calculation of the Euclidean distance-based EI criterion. The algorithm is able to significantly reduce the number of cells for the piecewise integration, thus reduce the computational time of the Euclidean distance-based EI criterion especially for higher number of objectives.

For the maximin distance-based EI criterion, Svenson *et al.* [28], [29] derived the formula for two objectives and recommended using Monte Carlo integration for higher number of objectives. However, the expression for the 2-objective case is not exactly in closed form, specifically, additional one-dimensional numerical quadrature is needed to finish the computation.

In terms of the hypervolume-based EI criterion, Emmerich *et al.* [18] initially suggested to use Monte Carlo integration to approximate the criterion. Recently, fast exact calculation algorithms have been proposed by Couckuyt *et al.* [30] and Hupkens *et al.* [31]. Both algorithms decompose the integration region into numerous regular cells and then combine the integration results of each cell. Couckuyt *et al.* [30] used the Walking Fish Group (WFG) algorithm to reduce the number of cells needed to calculate, however, no computational complexity was provided of this algorithm. Hupkens *et al.* [31] proposed a new computation scheme to calculate the hypervolume-based EI exactly and provided the upper bound of time complexity, $O(n^2)$ for 2-objective case and $O(n^3)$ for 3-objective case. The complexity of calculation of the hypervolume-based EI criterion is two fold. First, to do the piecewise integration, the integration region needs to be decomposed into $h \approx (k+1)^m$ regular cells. Second, for each cell, at least an m -dimensional hypervolume [31] or a $h \approx (k+1)^m$ times multiplications [30] needed to be calculated, which are computationally expensive. Although significant reduction of number of cells can be achieved [30], this approach does not escape the ‘curse of dimensionality’ with respect to the number of objectives.

C. Monotonicity Properties of the State-of-the-art Multiobjective EI Criteria

The monotonicity properties are thought to be fundamentally important for multiobjective infill criteria [22], [44]. The

two most important monotonicity properties are considered here. Given the objective prediction vectors $\hat{\mathbf{y}}^1, \hat{\mathbf{y}}^2$ and uncertainty vectors $\mathbf{s}^1, \mathbf{s}^2$ of two different points $\mathbf{x}^1, \mathbf{x}^2$, the properties are

- (N1) if $\mathbf{s}^1 = \mathbf{s}^2$ and $\hat{\mathbf{y}}^1 \prec \hat{\mathbf{y}}^2$, then $EI(\mathbf{x}^1) > EI(\mathbf{x}^2)$;
- (N2) if $\hat{\mathbf{y}}^1 = \hat{\mathbf{y}}^2$ and $\mathbf{s}^1 \succ \mathbf{s}^2$, then $EI(\mathbf{x}^1) > EI(\mathbf{x}^2)$.

In the single-objective EGO algorithm, the EI function is monotonously decreasing in $\hat{\mathbf{y}}$ and monotonously increasing in \mathbf{s} . In fact, the properties N1 and N2 require the multiobjective EI criteria be monotonously decreasing with respect to the prediction vector $\hat{\mathbf{y}}$ and monotonously increasing with respect to the uncertainty vector \mathbf{s} in terms of dominance measurement.

The maximin distance [29] and hypervolume-based (for 2-objective case) [44] EI criteria have been proven to be compliant with both of these two monotonicity properties. However, the Euclidean distance-based EI criterion is not compliant with these two monotonicity properties [22], which is thought to be the main disadvantage of this criterion.

IV. THE PROPOSED EXPECTED IMPROVEMENT MATRIX CRITERIA

The execution of the multiobjective EGO algorithm heavily depends on the computational time of the multiobjective EI criterion. For example, for a 6-objective problem, 200 iterations are required and an internal optimization of the multiobjective EI criterion is done by Genetic Algorithm (GA) with a population size of 100 and 100 generations (since the multiobjective EI function is highly multi-modal and nonlinear) for each iteration. Then a total $100 \times 100 \times 200 = 2000000$ evaluations of the multiobjective EI criterion is needed. Suppose that one evaluation of the 6-objective EI criterion through Monte Carlo integration or tedious piecewise integration needs one second, then the total evaluation time of the multiobjective EI criterion is

$$\frac{2000000 \times 1 \text{ seconds}}{60 \times 60 \times 24} \approx 23 \text{ days}, \quad (19)$$

which may even exceed the evaluation time of the computationally expensive black-box simulations.

The expensive computational cost limits the usage of the state-of-the-art multiobjective EI criteria in practice when dealing with many objective problems. Although there are computational cheap criteria such as the vector EI criterion [19], the weighted EI criteria [20], [21] and the SMS-EGO criterion [22] for many objective optimization, they often lack of theoretical properties. In this paper, we propose a new approach to build cheap-to-evaluate and still efficient multiobjective EI criteria based on the concept of the expected improvement matrix (EIM). The proposed EIM criteria are remarkably fast to compute since their computation scales linearly with the number of objectives and have better theoretical properties when compared to the previously proposed linear time EI criteria.

A. The Concept of the Expected Improvement Matrix

When dealing with multiobjective problem, the current best solution f_{\min} in single-objective optimization expands in two directions: the number of points in current best solution

increases from one to k ; the dimension of each point changes from one to m . For multiobjective optimization, the current best solution is in fact a two-dimensional matrix

$$\begin{bmatrix} f_1^1 & f_2^1 & \cdots & f_m^1 \\ f_1^2 & f_2^2 & \cdots & f_m^2 \\ \vdots & \vdots & \ddots & \vdots \\ f_1^k & f_2^k & \cdots & f_m^k \end{bmatrix}. \quad (20)$$

Inspired by this, the scalar function $EI(\mathbf{x})$ in single-objective optimization can also be expanded into a two-dimensional matrix for multiobjective optimization, specifically, the expected improvement matrix (EIM)

$$\begin{bmatrix} EI_1^1(\mathbf{x}) & EI_2^1(\mathbf{x}) & \cdots & EI_m^1(\mathbf{x}) \\ EI_1^2(\mathbf{x}) & EI_2^2(\mathbf{x}) & \cdots & EI_m^2(\mathbf{x}) \\ \vdots & \vdots & \ddots & \vdots \\ EI_1^k(\mathbf{x}) & EI_2^k(\mathbf{x}) & \cdots & EI_m^k(\mathbf{x}) \end{bmatrix}, \quad (21)$$

and

$$EI_i^j(\mathbf{x}) = (f_i^j - \hat{y}_i(\mathbf{x}))\Phi\left(\frac{f_i^j - \hat{y}_i(\mathbf{x})}{s_i(\mathbf{x})}\right) + s_i(\mathbf{x})\phi\left(\frac{f_i^j - \hat{y}_i(\mathbf{x})}{s_i(\mathbf{x})}\right), \quad (22)$$

where $i = 1, 2, \dots, m$ and $j = 1, 2, \dots, k$. The element $EI_i^j(\mathbf{x})$ in EIM represents the expected improvement of the studying point \mathbf{x} beyond the j th non-dominated front point in i th objective. A two-dimensional example of the EI matrix is given in Fig. 4. The j th row in the matrix $EI^j(\mathbf{x})$ represents the expected improvements beyond the j th non-dominated point in all objectives; the i th column in the matrix $EI_i(\mathbf{x})$ represents the expected improvement in i th objective beyond all the non-dominated points. In summary, the EIM contains all the information about the expected improvements of the studying point \mathbf{x} beyond all the non-dominated front points in all directions. More importantly, the expected improvement matrix stays in closed form, thus is cheap to calculate.

In fact, the EI matrix is a simple and natural idea when dealing with multiobjective problems. However, the EI matrix gives no comprehensive judgement about how much the studying point can improve the Pareto front approximation. In the following section, the proposed approach is described to aggregate the EI matrix into a scalar value to measure the expected improvement of the studying point compared against the current Pareto front approximation.

B. The Proposed Multiobjective EIM Criteria

The trick the proposed approach used is that it adopts the way of defining ‘the multiobjective improvement’ in the m -dimensional objective space to define ‘the multiobjective expected improvement’. In other words, replacing ‘the improvement’ in the multiobjective improvement functions by ‘the expected improvement’ can derive the corresponding EIM criteria. Specifically, replacing the term $f_i^j - y_i(\mathbf{x})$ in

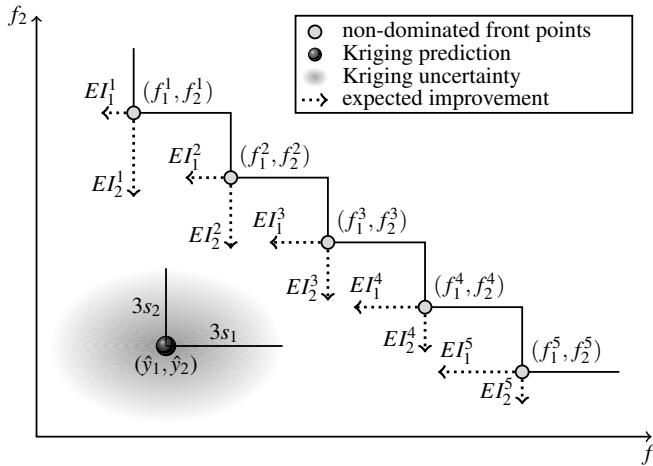


Fig. 4. A two-dimensional example of the expected improvement matrix.

the multiobjective improvement functions by the term $EI_i^j(\mathbf{x})$ derives the formulas of the EIM criteria.

For the Euclidean distance improvement in (13), its corresponding Euclidean distance-based EIM criterion is

$$EIM_e(\mathbf{x}) = \min_{j=1}^k \sqrt{\sum_{i=1}^m (EI_i^j(\mathbf{x}))^2}. \quad (23)$$

For consistency, the maximin distance improvement function in (14) can be rewritten as

$$I_m(\mathbf{x}) = \min_{j=1}^k \left[\max_{i=1}^m (f_i^j - y_i(\mathbf{x})) \right]. \quad (24)$$

Then the maximin distance-based EIM criterion can be given as

$$EIM_m(\mathbf{x}) = \min_{j=1}^k \left[\max_{i=1}^m EI_i^j(\mathbf{x}) \right]. \quad (25)$$

The hypervolume improvement function in (16) can not directly be used in the EIM criterion. Instead, a new modified hypervolume improvement function is proposed

$$I_{hm}(\mathbf{x}) = \min_{j=1}^k \left[H(f^j \cup p) - H(f^j) \right]. \quad (26)$$

The idea of the modified hypervolume improvement is explained in Fig. 5. In the figure, point j is an arbitrary point on the non-dominated front and point p is the studying point. The region filled with darker color indicates the hypervolume improvement of point p when only the point j is considered on the non-dominated front. Then we can calculate the k (k is the number of non-dominated front points) hypervolume improvements considering each point on the non-dominated front at one time. The modified hypervolume improvement is defined to be the minimum of the k hypervolume improvements. At first sight the modified hypervolume improvement seems more expensive to calculate, fortunately, the hypervolume improvement is analytic when only one non-dominated front point is considered. As a result, the modified hypervolume improvement of point $y(\mathbf{x})$ can be calculated in closed form

$$I_{hm}(\mathbf{x}) = \min_{j=1}^k \left[\prod_{i=1}^m (r_i - y_i(\mathbf{x})) - \prod_{i=1}^m (r_i - f_i^j) \right]. \quad (27)$$

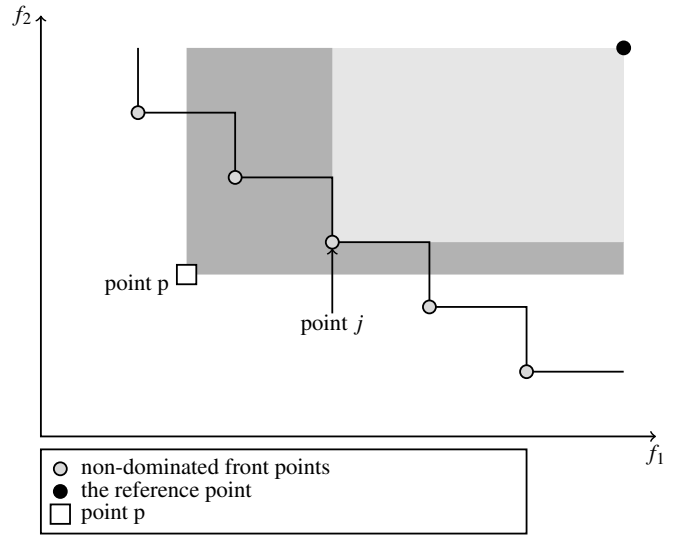


Fig. 5. The hypervolume improvement of point p beyond point j .

Notice that $-y_i(\mathbf{x}) = (f_i^j - y_i(\mathbf{x})) - f_i^j$, then the hypervolume-based EIM criterion can be given in closed form

$$EIM_h(\mathbf{x}) = \min_{j=1}^k \left[\prod_{i=1}^m (r_i + EI_i^j(\mathbf{x}) - f_i^j) - \prod_{i=1}^m (r_i - f_i^j) \right]. \quad (28)$$

It should be noted that the modified hypervolume improvement is not designed to replace the real hypervolume improvement. The only purpose of the proposition is to apply the hypervolume improvement into the EIM criterion.

C. Monotonicity Properties of the Proposed Multiobjective EIM Criteria

The monotonicity properties can be easily proven for the three proposed multiobjective EIM criteria. When condition N1 ($s^1 = s^2$ and $\hat{y}^1 \prec \hat{y}^2$), or N2 ($\hat{y}^1 = \hat{y}^2$ and $s^1 \succ s^2$) is met, it is easy to derive $EI_i^j(\mathbf{x}^1) > EI_i^j(\mathbf{x}^2)$ for $i = 1, 2, \dots, m$ and $j = 1, 2, \dots, k$, because the single-objective $EI(\mathbf{x})$ is monotonously decreasing in \hat{y} and monotonously increasing in s [6]. From the EIM criteria in (23), (25), and (28), it is obvious that when all the elements in the expected improvement matrix increase, the three EIM criteria will increase as well. Therefore we can get $EIM_e(\mathbf{x}^1) > EIM_e(\mathbf{x}^2)$, $EIM_m(\mathbf{x}^1) > EIM_m(\mathbf{x}^2)$ and $EIM_h(\mathbf{x}^1) > EIM_h(\mathbf{x}^2)$.

It is interesting to see that the Euclidean distance-based EI criterion is not compliant with the monotonicity properties but the Euclidean distance-based EIM criterion is compliant with the monotonicity properties. The reason is explained in Figs. 6 and 7. In the figures, we assume that point 1 has the minimum Euclidean distance improvement to both point A and point B among all the non-dominated front points. We also assume that point 1 has the minimum Euclidean distance expected improvement to both point A and point B among all the non-dominated front points. As a result, we only need to consider point 1 on the non-dominated front. In Figs. 6 and 7, compared to point 1, the improvements of point A and point B along objective f_1 are both negative and the improvement of point A is actually greater than point B along

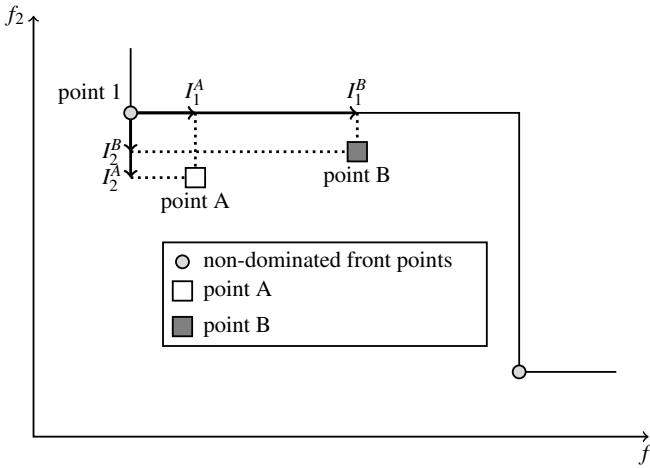


Fig. 6. An example of the Euclidean distance improvement.

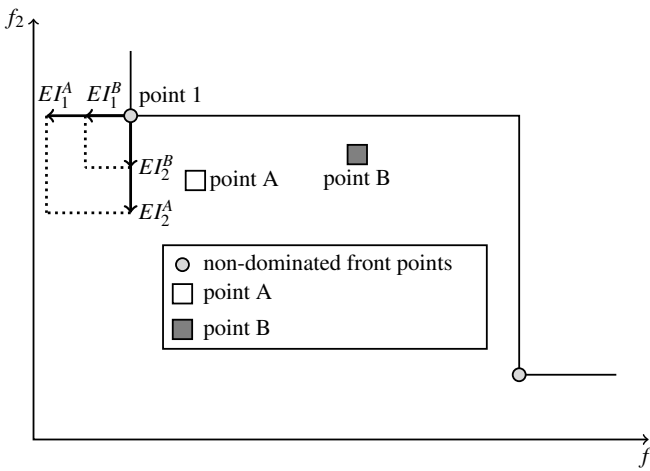


Fig. 7. An example of the expected Euclidean distance improvement.

objective f_1 . But the Euclidean distance improvement does not consider the direction of the improvement and takes the absolute value of the axis-wise improvement. Therefore, the Euclidean distance improvement will prefer point B over point A despite A dominating B. On the contrary, compared to point 1, the expected improvements of point A and point B along objective f_1 are both positive, as shown in Fig. 7. The expected improvement of point A is greater than point B, which makes the Euclidean distance-based EIM criterion choose point A over point B.

D. More Properties of the Proposed Multiobjective EIM Criteria

It is easy to see that when the number of objectives m is equal to one, the EI matrix deteriorates to a single scalar and the EIM criteria deteriorate to the single-objective EI criterion. This means the single-objective EI criterion is a special case of the proposed multiobjective EIM criteria.

When the studying point is the same as one of the sampled points so far, the uncertainty around the studying point would be zero, as in $s = 0$ in (7), and thus the EI would be zero.

Obviously, when all the EI values in the EI matrix are zeros, the value of EIM criteria in (23), (25), and (28) would be zero too. On the contrary, if the studying point is not the same as any of the sampled points, the uncertainty of the studying point would be positive, as in $s > 0$ in (7), and thus the EI would be positive. When all the EI values in EI matrix are positive, the EIM criteria would be positive as a result. This means that the next point selected by the EIM criteria to evaluate would be anywhere but the sampled points. As a consequence, the iterative sampling based on the EIM criteria is dense and the convergence of the EIM approach can be guaranteed according to the theory of [45]. However this property is only true for noise-free functions. If the function evaluation is noisy, there would be a non-zero uncertainty associated with any studying point from the Gaussian process model and the convergence can not be guaranteed.

The EI values in the EI matrix can be computed in parallel, which can further increase the computational speed of the proposed EIM criteria. In terms of the implementations of the multiobjective EIM criteria, matrix operation provided by some softwares like MATLAB® can ease and accelerate the calculation more.

E. A 2-objective Example of the Multiobjective EI and EIM Criteria

First, we compare the multiobjective EI criteria and EIM criteria on the 2-objective ZDT1 function [46]. We calculate the 2-objective EI and EIM criteria, and plot the contours in the two-dimensional design space, as shown in Fig. 8. In these figures, the dots present the 10 sampled points, the color of the contours indicates the value of the criteria. The darker the color the higher the value. It is interesting to find that although the proposed EIM criteria are developed in a very different way as the traditional multiobjective EI criteria, the contours of the EIM criteria have very similar trends to their corresponding EI criteria. The plot of the maximin distance-based EIM criterion is almost the same as the maximin distance-based EI criterion. The Euclidean distance-based and hypervolume based EIM criteria are different from the corresponding EI criteria, but they suggest approximatively the same candidate for evaluation.

V. NUMERICAL EXPERIMENTS

A. Test Suites

The (multiobjective) EGO algorithm has poor performance on objective functions which are difficult for the Kriging model to approximate [30]. These difficult functions are often extremely multi-modal or have huge objective region that are hard for the Kriging model to capture the behavior with a small set of design points. Therefore, test problems with fine objectives are selected here to study the proposed EIM criteria compared against the state-of-the-art EI criteria. For 2-objective problems, the ZDT1, ZDT2, and ZDT3 functions from the ZDT test suite [46] are selected. The DTLZ2, DTLZ5, and DTLZ7 functions from the DTLZ test suite [47] with three, four and six objectives are used in the experiment to study the infill criteria's ability to deal with large number

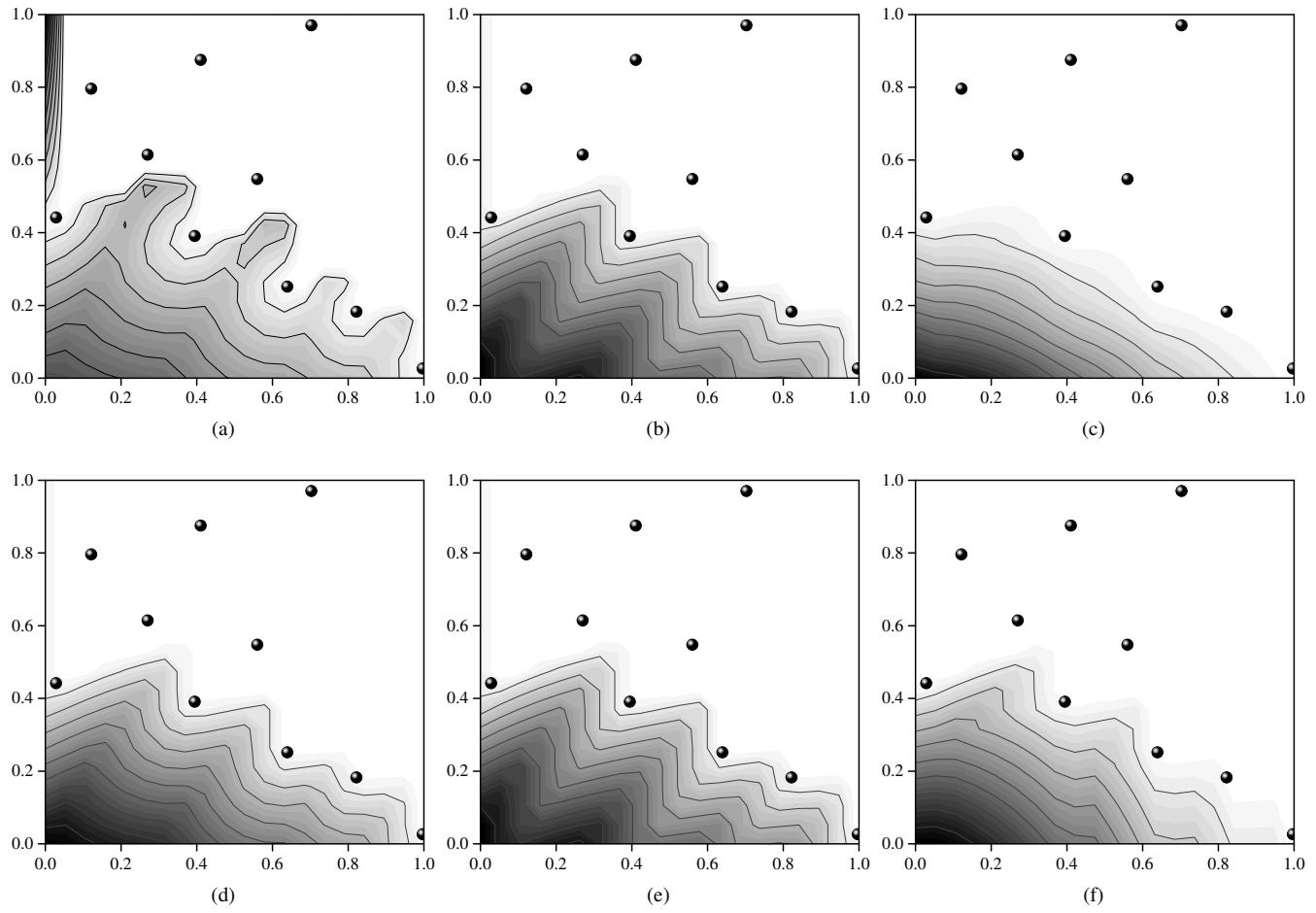


Fig. 8. Plots of multiobjective EI and EIM criteria in the design space of ZDT1 problem. (a) EI_e ; (b) EI_m ; (c) EI_h ; (d) EIM_e ; (e) EIM_m ; (f) EIM_h .

of objectives. The selected test problems contain various types of Pareto fronts: convex fronts (ZDT1), concave fronts (ZDT2 and DTLZ2), disconnected fronts (ZDT3 and DTLZ7) and curve-shape fronts (DTLZ5).

B. Experiment Settings

(1) Test Settings

- a) The number of design variables n is set to be 6.
- b) The number of initial design points is set to be $11n - 1 = 65$.
- c) The maximal number of function evaluation is 100 for $m = 2$ and 200 for $m \in \{3, 4, 6\}$.
- d) The number of independent runs is 10.

(2) Building Kriging Model

The DACE toolbox [48] is used for building the Kriging model in the experiments with the following settings:

- a) The regression function is set to be *regpoly0*.
- b) The correlation function is set to be *corrgauss*.
- c) The initial values of θ_i ($i = 1, 2, \dots, n$) is set to be 1.
- d) The region of θ_i ($i = 1, 2, \dots, n$) is set to be $[10^{-3}, 10^3]$.

(3) Implementations of Multiobjective EI Criteria

- a) For the Euclidean distance-based EI criterion, the fast exact calculation algorithm of Couckuyt *et al.* [30] is used for all test problems. The code is available in the

SUMO (SURrogate MOdeling) toolbox [49], and the specific code for 64 bit Windows machine is kindly provided by the first author of [30].

- b) For the maximin distance-based EI criterion, the 2-objective function is implemented according the formula [29] and Monte Carlo integrations with 1000 points are used for higher objective problems.
- c) For the hypervolume-based EI criterion, the fast exact code calculation algorithm of Couckuyt *et al.* [30] is used for all test problems. The code is also kindly provided by the first author of [30].
- d) The MATLAB[®] code of the three proposed EIM used in the experiments are given in Appendix A.
- (4) Optimizer of the multiobjective EI criteria
The Differential Evolution algorithm [50], [51] is used to find the maximum of all the compared multiobjective infill criteria with the following settings:
 - a) The population size is set to be 50.
 - b) The maximum iterations is set to be 50.
 - c) The step size in DE is set to be 0.8.
 - d) The crossover probability is set to be 0.8.
 - e) The strategy is set to be *DE/rand/1/bin*.
 - f) The DE algorithm is repeated 4 times to find the best solution.
- (5) Other settings

TABLE I
THE REFERENCE POINT FOR CALCULATING THE HYPERVOLUME OF EACH TEST PROBLEM

instance	m	Reference point
ZDT1	2	(11,11)
ZDT2	2	(11,11)
ZDT3	2	(11,11)
DTLZ2	3	(2.5,2.5,2.5)
DTLZ2	4	(2.5,2.5,2.5,2.5)
DTLZ2	6	(2.5,2.5,2.5,2.5,2.5,2.5)
DTLZ5	3	(2.5,2.5,2.5)
DTLZ5	4	(2.5,2.5,2.5,2.5)
DTLZ5	6	(2.5,2.5,2.5,2.5,2.5,2.5)
DTLZ7	3	(30,30,30)
DTLZ7	4	(50,50,50,50)
DTLZ7	6	(70,70,70,70,70,70)

- a) All the objective functions are scaled into $[0, 1]$ using the minima and maxima of the objectives. When using the hypervolume-based EI and EIM criteria, the reference point is set to $r_i = 1.1$ for $i = 1, 2, \dots, m$.
- b) The Pareto set is identified from all the design points using the implementation of <http://www.mathworks.com/matlabcentral/fileexchange/17251-pareto-front>.
- c) If the updating point is too close to an existing point (Euclidean distance is small than 10^{-8}), it is replaced by maximizing the uncertainty of the Kriging model to avoid ill conditioning when building the Kriging model.

C. Compared metrics

The hypervolume indicator [35] is used to measure the quality of the resulting Pareto front approximations. The hypervolume can capture the closeness of the obtained solutions to the Pareto front as well as the spread property of the solutions. The reference points used for calculating the hypervolume values are set in Table I for each test problem.

In addition, the inverted generational distance (IGD) indicator [52] is used in this work to measure the convergence of the solution. Let P^* be Pareto front and P be the obtained Pareto front approximation, the IGD is defined as:

$$IGD = \frac{\sum_{p \in P^*} d(p, P)}{|P^*|}, \quad (29)$$

where $d(\cdot)$ is the minimum Euclidean distance measurement. In order to have a lower value of IGD, the Pareto front approximation P should be very close to the Pareto front P^* and can not miss any part of P^* .

The Pareto fronts of these test problems are known. The Pareto set for ZDT problems are $x_i = 0$ ($i = 2, 3, \dots, n$); the Pareto set for DTLZ2 and DTLZ5 are $x_i = 0.5$ ($i = m, m+1, \dots, n$); the Pareto set for DTLZ7 are $x_i = 0$ ($i = m, m+1, \dots, n$). The Pareto fronts of the test problems can be represented by uniformly distributed grid points in the rest of the design space. The grid points are set to be 101 for ZDT test problems, 51×51 for 3-objective DTLZ problems, $21 \times 21 \times 21$ for 4-objective DTLZ problems and $11 \times 11 \times 11 \times 11 \times 11$ for 6-objective DTLZ problems.

VI. RESULTS

The hypervolume indicator and the IGD indicator of the Pareto front approximations obtained by each multiobjective EI infill criteria are calculated. The statistical values, specifically the median, average and the standard derivation (s.t.d.) of the ten independent runs of the hypervolume and IGD indicator are given respectively. In addition, both the paired *t*-test and the Wilcoxon signed rank test are applied to identify whether the means and medians of the results obtained by one multiobjective EIM criterion are significantly different from the results obtained by the corresponding multiobjective EI criterion. The *p*-values of the two significant tests are given (p_1 for the paired *t*-test and p_2 for the Wilcoxon signed rank test). If the *p*-value is smaller than the significant level of $\alpha = 0.05$, the significant difference is identified, then the significantly better value, that is the greater hypervolume value or the smaller IGD value, is boldfaced.

A. Results of ZDT test problems

Table II presents the results of the three ZDT test instances. Figs. 9-11 show the final Pareto front approximation by each algorithm with the lowest hypervolume of the ten runs on the ZDT test problems.

It is evident that the EI_e criterion is significantly worse than the other five criteria on all three ZDT test problems with respect to both the hypervolume and IGD indicators. Since the EI_e criterion does not have the monotonicity properties, it is not able to improve the current Pareto front approximation constantly during the iterations, thus derives poor results.

No significant difference is detected between the EI_m criterion and the EIM_m criterion, and between the EI_h criterion and the EIM_h criterion at the significant level of $\alpha = 0.05$. This indicates that the efficiencies of the two proposed EIM criteria are competitive to the two corresponding multiobjective EI criteria over the three 2-objective ZDT test instances.

Figs. 9-11 show the final Pareto front approximations produced by the compared infill criteria with the lowest hypervolume value in the ten runs. It can be seen that both the multiobjective EI and EIM criteria obtain very good Pareto front approximations on ZDT1 and ZDT2 problems, but relatively worse Pareto front approximations on ZDT3 problem. All the algorithms miss the last discrete Pareto front of the ZDT3 problem, and the EIM_h criterion misses the last two discrete Pareto fronts. It seems that the Euclidean distance and maximin distance improvement functions have more advantages than the hypervolume improvement function in terms of finding discrete Pareto fronts. Overall, the 2-objective EIM criteria have competitive performances compared with the 2-objective EI criteria on the three ZDT test problems.

B. Results of DTLZ2 test problems

The DTLZ2 test problem can investigate the ability of a multiobjective optimization algorithm to scale up its performance in large number of objectives. Table III shows the results of the compared multiobjective infill criteria over the DTLZ2 instance with 3, 4 and 6 objectives. Fig. 12 illustrates

TABLE II
THE STATISTICS OF THE HYPERVOLUME AND IGD VALUES OF THE PARETO FRONT APPROXIMATIONS OBTAINED BY THE COMPARED MULTIOBJECTIVE INFILL CRITERIA, AND THE p -VALUES OF THE SIGNIFICANT TESTS ON ZDT TEST PROBLEMS

indicator	instance		EI_e	EIM_e	EI_m	EIM_m	EI_h	EIM_h
hypervolume	ZDT1	median	120.35	120.64	120.64	120.64	120.64	120.64
		mean	120.11	120.64	120.64	120.63	120.64	120.64
		s.t.d	0.6381	0.0113	0.0132	0.0304	0.0042	0.0033
		(p_1, p_2)	(0.0020, 0.0351)		(0.1055, 0.1958)		(0.1602, 0.2400)	
	ZDT2	median	120.00	120.30	120.30	120.30	120.30	120.30
		mean	118.80	120.30	120.30	120.30	120.30	120.30
		s.t.d	2.3554	0.0051	0.0035	0.0049	0.0031	0.0057
		(p_1, p_2)	(0.0020, 0.0888)		(0.1602, 0.1617)		(0.4316, 0.2797)	
	ZDT3	median	114.10	128.24	128.36	128.50	128.24	127.94
		mean	115.31	127.89	127.99	127.91	127.77	126.38
		s.t.d	5.6419	1.3416	0.9626	1.1899	0.9922	3.0610
		(p_1, p_2)	(0.0020, 0.0001)		(1.0000, 0.7325)		(0.4316, 0.2170)	
IGD	ZDT1	median	0.1521	0.0181	0.0182	0.0207	0.0226	0.0215
		mean	0.1663	0.0178	0.0182	0.0202	0.0218	0.0211
		s.t.d	0.0779	0.0037	0.0018	0.0032	0.0026	0.0028
		(p_1, p_2)	(0.0020, 0.0002)		(0.1602, 0.1740)		(0.6953, 0.6945)	
	ZDT2	median	0.1630	0.0374	0.0288	0.0300	0.0309	0.0334
		mean	0.1737	0.0380	0.0303	0.0309	0.0313	0.0334
		s.t.d	0.0452	0.0071	0.0058	0.0056	0.0041	0.0053
		(p_1, p_2)	(0.0020, 0.0000)		(0.6250, 0.7335)		(0.5566, 0.3624)	
	ZDT3	median	0.6896	0.0380	0.0478	0.0418	0.0580	0.0564
		mean	0.6848	0.0425	0.0474	0.0468	0.0615	0.0739
		s.t.d	0.2288	0.0160	0.0166	0.0154	0.0219	0.0483
		(p_1, p_2)	(0.0020, 0.0000)		(0.9219, 0.9234)		(0.9219, 0.4373)	

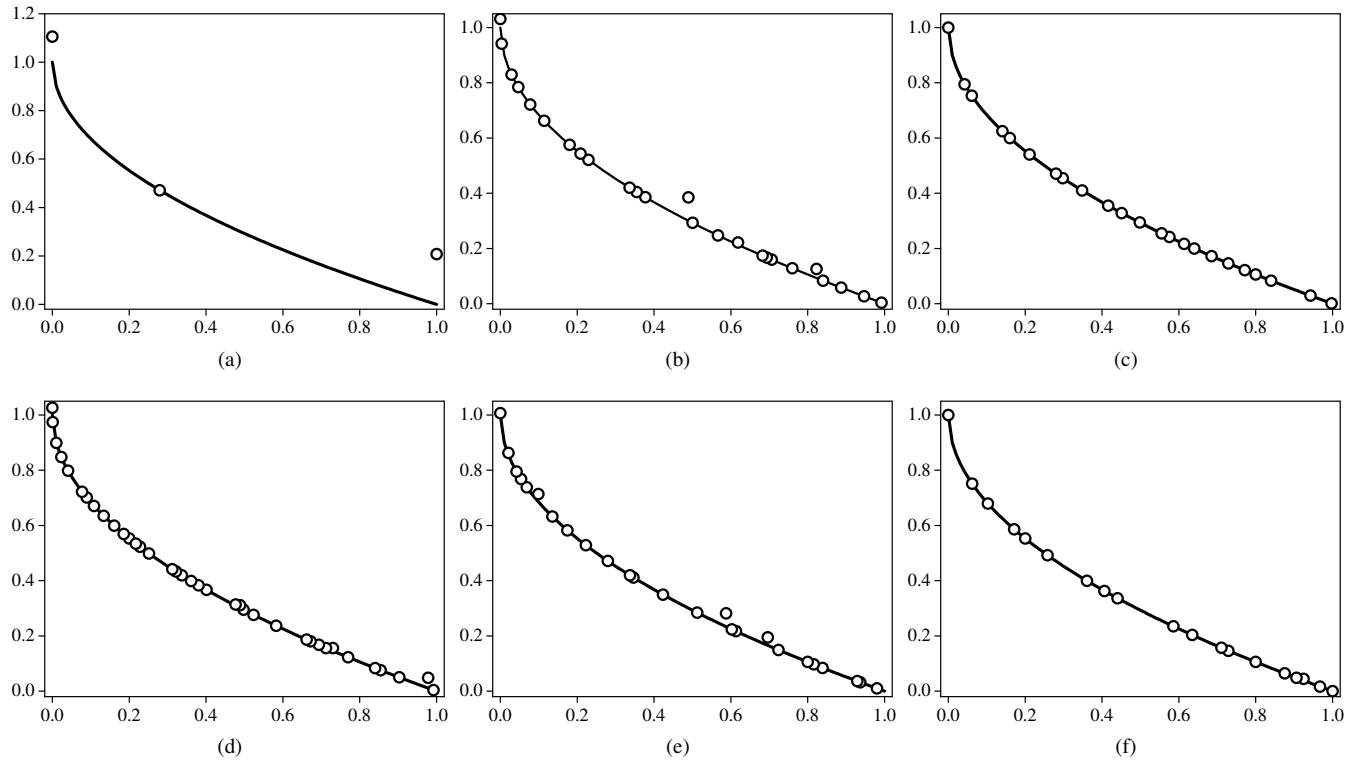


Fig. 9. Plots of the final Pareto front approximation obtained by each algorithm with the lowest hypervolume value in the 10 runs on ZDT1 problem. (a) EI_e ; (b) EI_m ; (c) EI_h ; (d) EIM_e ; (e) EIM_m ; (f) EIM_h .

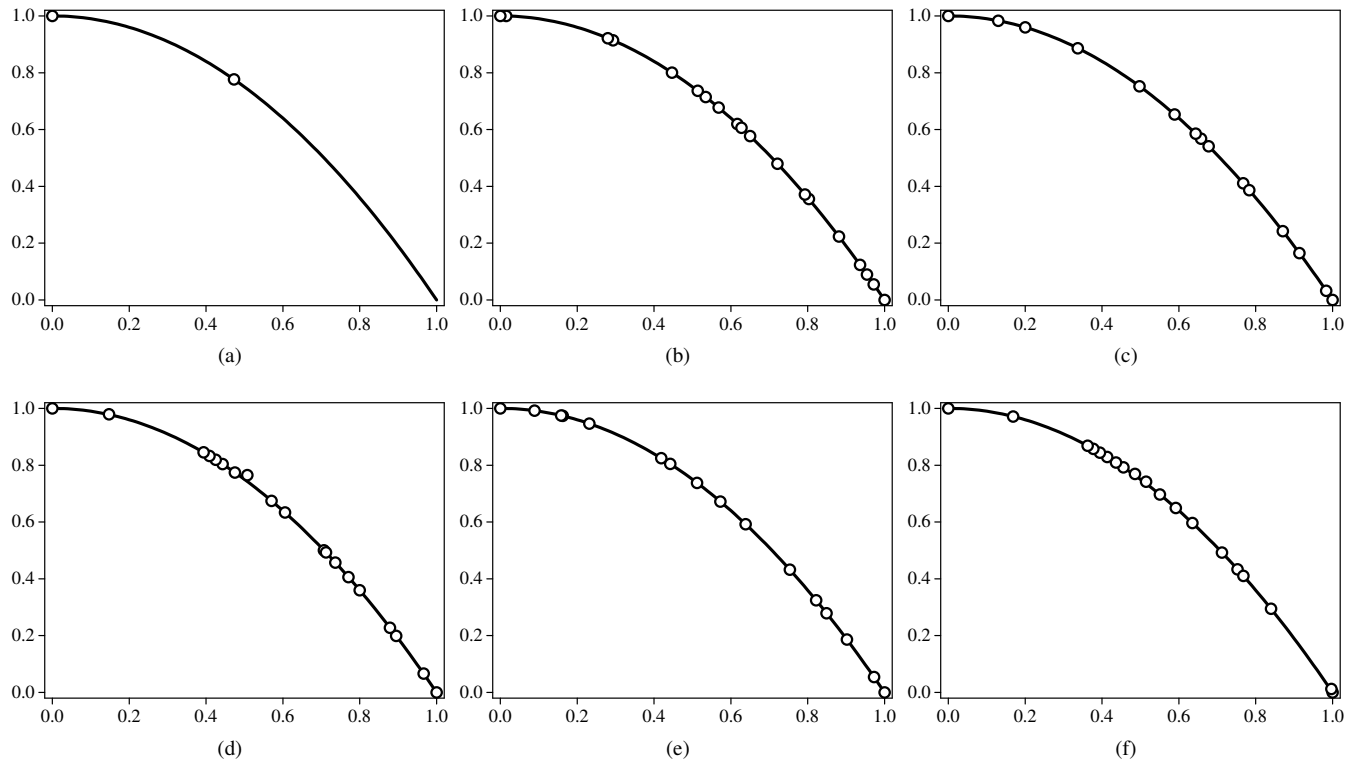


Fig. 10. Plots of the final Pareto front approximation obtained by each algorithm with the lowest hypervolume value in the 10 runs on ZDT2 problem. (a) EI_e ; (b) EI_m ; (c) EI_h ; (d) EIM_e ; (e) EIM_m ; (f) EIM_h .

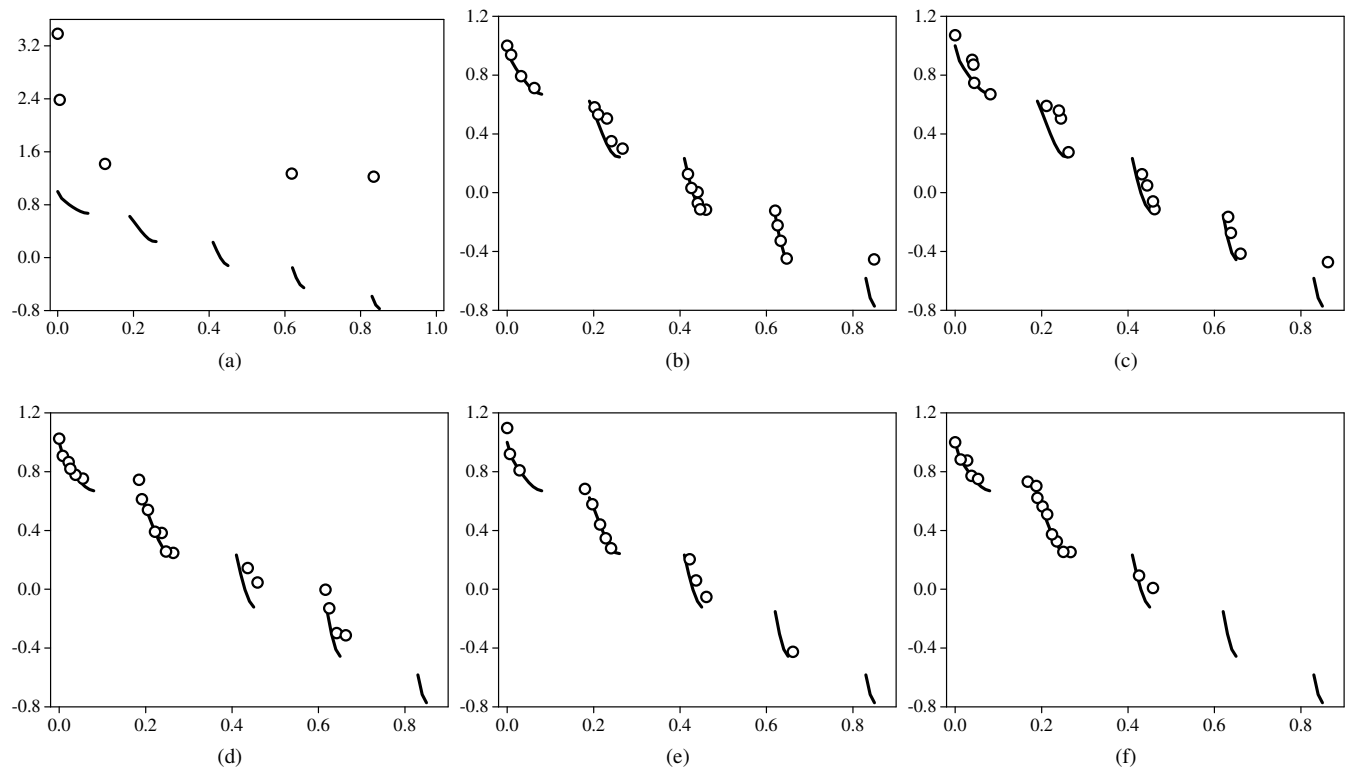


Fig. 11. Plots of the final Pareto front approximation obtained by each algorithm with the lowest hypervolume value in the 10 runs on ZDT3 problem. (a) EI_e ; (b) EI_m ; (c) EI_h ; (d) EIM_e ; (e) EIM_m ; (f) EIM_h .

the final Pareto front approximation by each criterion with the lowest hypervolume of the ten runs on the 3-objective DTLZ2 problem.

It can be seen from Fig. 12 that the final Pareto front approximation of the EI_e criterion is far from the Pareto front of the 3-objective DTLZ2 function. The EI_h criterion finds many points on the edges but few in the inner portion of the Pareto front. In comparison, the EI_m criterion produces the highest quality Pareto front approximation on the 3-objective DTLZ2 function among the three multiobjective EI criteria. The average hypervolume value of the EI_m criterion is 15.024 and are 14.645 and 14.961 for the EI_e and EI_h respectively.

On the other hand, all the three EIM criteria produce well-distributed Pareto front approximations on the 3-objective DTLZ2 problem (see Fig. 12). The hypervolume values of the EIM criteria are significantly larger than the corresponding EI criteria on the 3-objective DTLZ2 problem. Although the modified hypervolume improvement used in the EIM_h criterion is not the real hypervolume improvement, it seems to work fine to produce well-distributed Pareto front approximation on the DTLZ2 test problems.

When the number of objectives becomes high, the performance of the three EIM criteria are still competitive and even better compared against the state-of-the-art EI criteria. This indicates that the proposed EIM criteria are able to deal with problems with large number of objectives.

C. Results of DTLZ5 test problems

The DTLZ5 test problem can test the ability of a multiobjective optimization algorithm to converge to a curve. Table IV shows the results of the compared multiobjective infill criteria over the DTLZ5 instance with 3, 4 and 6 objectives. Fig. 13 illustrates the final Pareto front approximation by each criterion with the lowest hypervolume of the ten runs on the 3-objective DTLZ5 problem.

It shows in Fig. 13 that the three EIM criteria have no problem to converge to the curve of the Pareto front. The three EIM criteria outperform or perform similarly to the corresponding EI criteria on the 3-objective DTLZ5 test instance. The EIM_e outperforms the EI_e criteria significantly, and the EIM_h finds more Pareto front approximation points on the curve than the EI_h criterion. The efficiency of the EIM_m criterion is similar to the EI_m criterion on the 3-objective DTLZ5 test problem.

The ability of the EIM criteria to find the curve-shape Pareto front also scales up with the number of objectives on the DTLZ5 problems.

D. Results of DTLZ7 test problems

The DTLZ7 test problem can test the ability of a multiobjective optimization algorithm to maintain subpopulation of different regions. Table V shows the results of the compared multiobjective infill criteria over the DTLZ7 instance with 3, 4 and 6 objectives. Fig. 14 illustrates the final Pareto front approximation by each criterion with the lowest hypervolume of the ten runs on the 3-objective DTLZ7 problem.

It can be seen in Fig. 14 that the EIM_e and EIM_m criteria obtain fine discrete Pareto front approximations on the 3-objective DTLZ7 problem, and the EIM_h criterion produces

relatively worse Pareto front approximation. The EIM_h criterion finds a large amount of points on the first piece of the Pareto front but only few points on the last piece of the discrete Pareto front. This may indicate that the modified hypervolume improvement is good at finding continuous Pareto front but bad at maintaining multiple discrete Pareto fronts. The EI_h criterion also has trouble to maintain multiple discrete Pareto fronts of the DTLZ7 problem. The points on the last piece of the discrete Pareto front found by the EI_h are significantly fewer than the EIM_e , EIM_m and EI_m criteria. This indicates that the hypervolume improvement is less efficient than the Euclidean distance improvement and the maximin distance improvement in identifying multiple discrete Pareto fronts, which is also found on the ZDT3 test function.

The EIM_e and EIM_m criteria remain efficient as the number of objectives goes up on the DTLZ7 problems. It is recommended to use the EIM_e and EIM_m on problems that may have discrete Pareto fronts.

VII. THE COMPUTATION TIME

The main advantage of the proposed multiobjective EIM criteria is that they are much cheaper to evaluate than the state-of-the-art multiobjective EI criteria. This work also compares the computational time between the proposed EIM criteria and the state-of-the-art EI criteria. For all the experiments, the Kriging prediction vector and variance vector are fixed to $\mu_i = 10$ and $s_i = 2.5$ for all $i = 1, 2, \dots, m$. The convex Pareto fronts are generated using the method of [53]. The hardware is CPU: Intel(R) Core(TM) i7-6700 3.4GHz, RAM: 32GB 2400MHz. The software used is Microsoft Windows 10, 64 bit, MATLAB® (R2012b).

The three multiobjective EIM criteria used in the competition are given in Appendix A. For the Euclidean distance-based EI criterion, the current fastest code by Couckuyt *et al.* [30] (kindly provided by the first author of [30]) is used for the comparison. For the maximin distance-based EI criterion, the exact calculation code for two objectives is implemented in MATLAB according to the formula [29] and there is no exact calculation algorithm available for three and higher objectives so far. For the hypervolume-based EI criterion, both the fast codes of Hupkens *et al.* [31] (2-dimensional and 3-dimensional, available at <http://moda.liacs.nl/index.php?page=code>) and Couckuyt *et al.* [30] (kindly provided by the first author of [30]) are included in the competition. All the codes are validated using Monte Carlo simulations and the hypervolume-based EI code by Hupkens *et al.* [31] is validated against the code by Couckuyt *et al.* [30].

The results are displayed in Figs. 15-17, where EI_e -WFG and EI_h -WFG present the fast algorithms of the Euclidean distance-based and hypervolume-based EI criteria by Couckuyt *et al.* [30], and EI_h -IRS presents the fast algorithm of the hypervolume-based EI criterion by Hupkens *et al.* [31]. The shown computational time is the average value of 1000 runs (in seconds).

The computational time of the three EIM criteria is significantly smaller than their corresponding EI criteria for all the test instances. In Fig. 15, when there is only 10 non-dominated

TABLE III

THE STATISTICS OF THE HYPERVOLUME AND IGD VALUES OF THE PARETO FRONT APPROXIMATIONS OBTAINED BY THE COMPARED MULTIOBJECTIVE INFILL CRITERIA, AND THE p -VALUES OF THE SIGNIFICANT TESTS ON DTLZ2 TEST PROBLEMS

indicator	m		EI_e	EIM_e	EI_m	EIM_m	EI_h	EIM_h
hypervolume	3	median	14.665	15.026	15.023	15.027	14.961	15.031
		mean	14.645	15.026	15.024	15.026	14.961	15.031
		s.t.d (p_1, p_2)	0.0829	0.0016	0.0017	0.0019	0.0168	0.0013
	4	median	38.068	38.613	38.609	38.609	38.469	38.630
		mean	38.035	38.612	38.609	38.607	38.476	38.630
	6	median	243.54	243.88	243.85	243.86	243.39	243.84
		mean	243.53	243.88	243.85	243.85	243.35	243.81
		s.t.d (p_1, p_2)	0.0382	0.0131	0.0317	0.0320	0.4164	0.1200
IGD	3	median	0.1935	0.0631	0.0655	0.0626	0.1379	0.0616
		mean	0.1898	0.0634	0.0659	0.0634	0.1418	0.0614
		s.t.d (p_1, p_2)	0.0190	0.0013	0.0017	0.0034	0.0174	0.0024
	4	median	0.2244	0.1231	0.1246	0.1217	0.1989	0.1131
		mean	0.2224	0.1237	0.1249	0.1219	0.1992	0.1116
		s.t.d (p_1, p_2)	0.0085	0.0033	0.0037	0.0037	0.0045	0.0029
	6	median	0.1944	0.1732	0.1748	0.1711	0.1881	0.1605
		mean	0.1946	0.1721	0.1745	0.1723	0.1885	0.1600
		s.t.d (p_1, p_2)	0.0027	0.0025	0.0029	0.0037	0.0025	0.0027

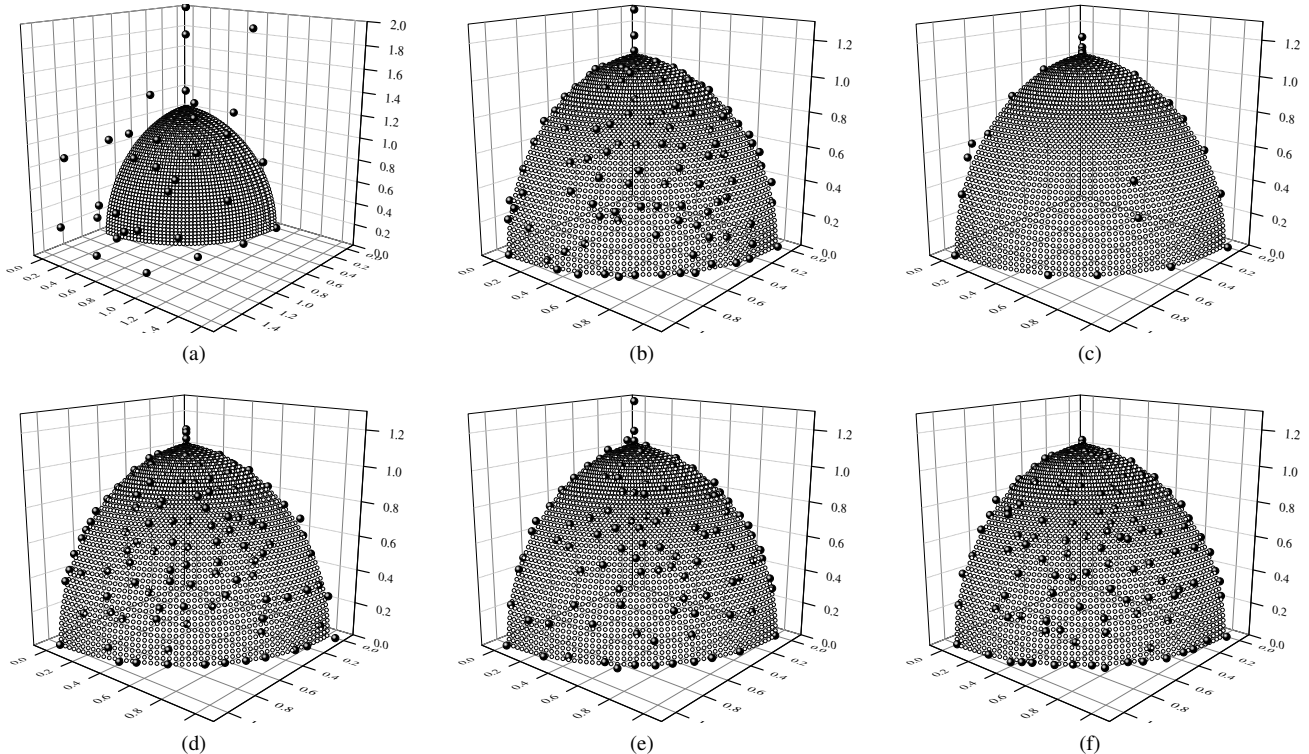


Fig. 12. Plots of the final Pareto front approximation obtained by each algorithm with the lowest hypervolume value in the 10 runs on DTLZ2 problem. (a) EI_e ; (b) EI_m ; (c) EI_h ; (d) EIM_e ; (e) EIM_m ; (f) EIM_h .

TABLE IV

THE STATISTICS OF THE HYPERVOLUME AND IGD VALUES OF THE PARETO FRONT APPROXIMATION OBTAINED BY THE COMPARED MULTIOBJECTIVE INFILL CRITERIA, AND THE p -VALUES OF THE SIGNIFICANT TESTS ON DTLZ5 TEST PROBLEMS

indicator	m		EI_e	EIM_e	EI_m	EIM_m	EI_h	EIM_h
hypervolume	3	median	12.649	13.118	13.112	13.116	13.097	13.123
		mean	12.611	13.118	13.114	13.118	13.097	13.123
		s.t.d (p_1, p_2)	0.1422	0.0037	0.0064	0.0044	0.0071	0.0032
	4	median	31.681	32.455	32.447	32.448	32.268	32.491
		mean	31.670	32.451	32.440	32.439	32.270	32.486
		s.t.d (p_1, p_2)	0.1692	0.0178	0.0150	0.0231	0.0799	0.0217
IGD	6	median	197.26	198.32	198.08	198.26	195.75	197.98
		mean	197.19	198.32	198.09	198.22	195.96	197.79
		s.t.d (p_1, p_2)	0.3612	0.0664	0.0077	0.1062	0.6926	0.5922
	3	median	0.1159	0.0219	0.0220	0.0210	0.0294	0.0209
		mean	0.1241	0.0225	0.0225	0.0216	0.0305	0.0208
		s.t.d (p_1, p_2)	0.0202	0.0023	0.0026	0.0024	0.0036	0.0017
	4	median	0.0904	0.0346	0.0358	0.0327	0.0301	0.0220
		mean	0.0906	0.0334	0.0352	0.0337	0.0293	0.0206
		s.t.d (p_1, p_2)	0.0074	0.0037	0.0040	0.0047	0.0032	0.0030
	6	median	0.0288	0.0183	0.0218	0.0187	0.0073	0.0108
		mean	0.0292	0.0176	0.0214	0.0192	0.0077	0.0111
		s.t.d (p_1, p_2)	0.0050	0.0033	0.0043	0.0036	0.0022	0.0031

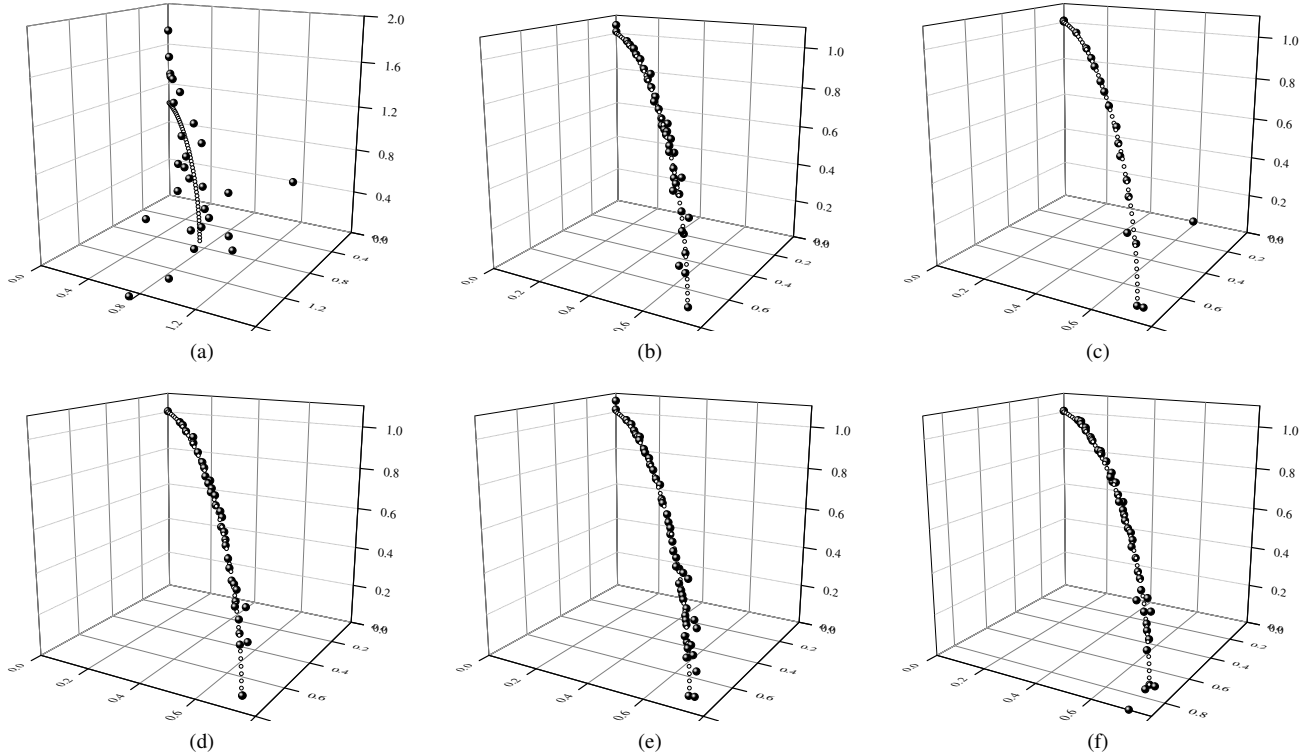


Fig. 13. Plots of the final Pareto front approximation obtained by each algorithm with the lowest hypervolume value in the 10 runs on DTLZ5 problem. (a) EI_e ; (b) EI_m ; (c) EI_h ; (d) EIM_e ; (e) EIM_m ; (f) EIM_h .

TABLE V

THE STATISTICS OF THE HYPERVOLUME AND IGD VALUES OF THE PARETO FRONT APPROXIMATION OBTAINED BY THE COMPARED MULTIOBJECTIVE INFILL CRITERIA, AND THE p -VALUES OF THE SIGNIFICANT TESTS ON DTLZ7 TEST PROBLEMS

indicator	m		EI_e	EIM_e	EIm	EIM_m	EI_h	EIM_h
hypervolume	3	median	6412.9	6908.4	6875.6	6876.0	6899.3	6883.2
		mean	6464.0	6899.8	6877.8	6873.5	6897.1	6837.9
		s.t.d	169.44	16.348	22.258	32.308	13.386	82.371
		(p_1, p_2)	(0.0020, 0.0000)		(0.7695, 0.6372)		(0.1309, 0.0596)	
	4	median	5.63×10^6	5.81×10^6	5.83×10^6	5.81×10^6	5.76×10^6	5.65×10^6
		mean	5.64×10^6	5.80×10^6	5.80×10^6	5.78×10^6	5.77×10^6	5.65×10^6
		s.t.d	3.41×10^4	3.84×10^4	7.11×10^4	6.01×10^4	6.64×10^4	6.72×10^4
	6	median	1.06×10^{11}	1.09×10^{11}	1.08×10^{11}	1.07×10^{11}	1.05×10^{11}	1.04×10^{11}
		mean	1.06×10^{11}	1.08×10^{11}	1.08×10^{11}	1.08×10^{11}	1.05×10^{11}	1.04×10^{11}
		s.t.d	7.31×10^8	1.82×10^8	1.36×10^9	1.24×10^9	1.00×10^9	8.39×10^8
		(p_1, p_2)	(0.0020, 0.0000)		(0.1934, 0.0932)		(0.0020, 0.0067)	
IGD	3	median	0.4311	0.0554	0.0631	0.0625	0.0858	0.0702
		mean	0.4314	0.0568	0.0624	0.0621	0.0846	0.0710
		s.t.d	0.0630	0.0039	0.0033	0.0039	0.0043	0.0051
		(p_1, p_2)	(0.0020, 0.0000)		(0.8457, 0.8912)		(0.0020, 0.0000)	
	4	median	0.5785	0.2008	0.2096	0.2151	0.1912	0.3140
		mean	0.5635	0.2032	0.2287	0.2244	0.1905	0.3232
		s.t.d	0.0421	0.0177	0.0544	0.0436	0.0148	0.0916
	6	median	0.8950	0.5491	0.5773	0.5960	0.6351	0.8635
		mean	0.9004	0.5539	0.5729	0.6039	0.6363	0.9020
		s.t.d	0.0699	0.0551	0.0553	0.0720	0.0505	0.1767
		(p_1, p_2)	(0.0020, 0.0000)		(0.2324, 0.2213)		(0.0020, 0.0008)	

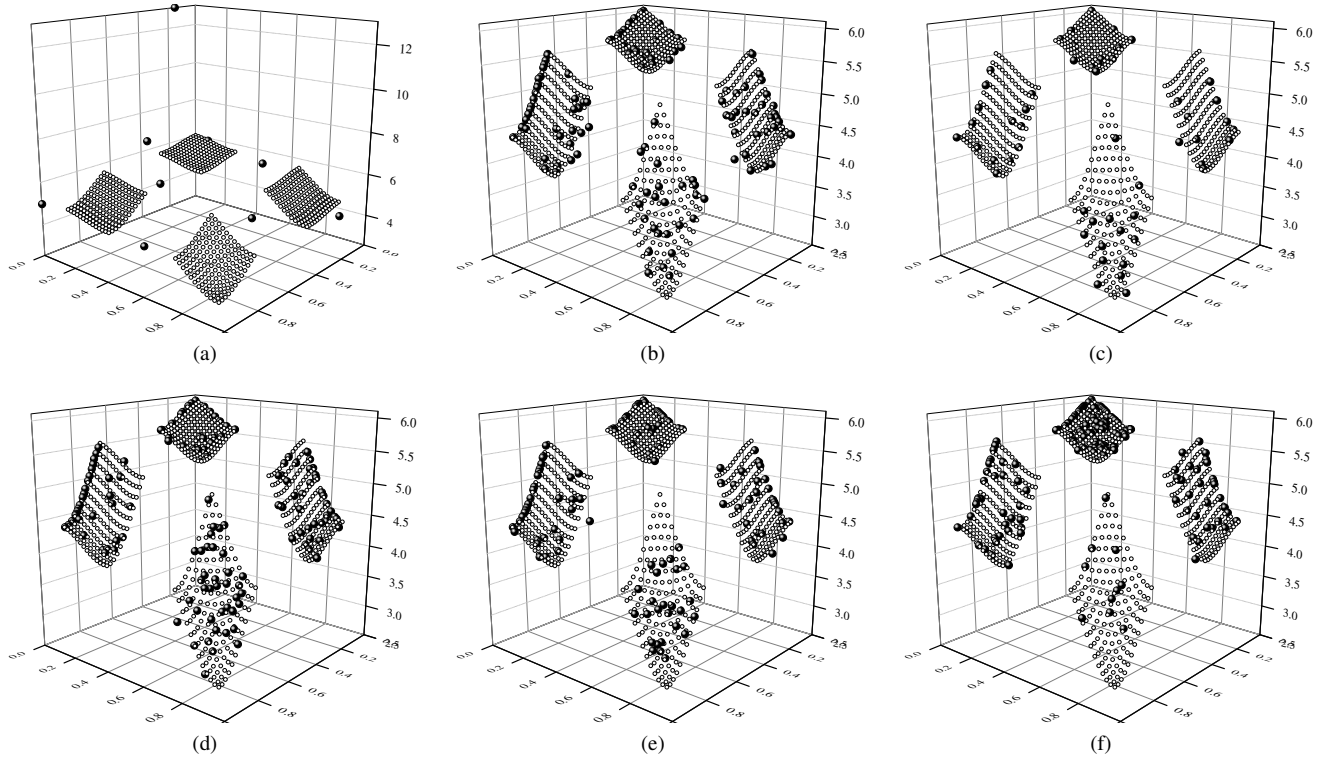


Fig. 14. Plots of the final Pareto front approximation obtained by each algorithm with the lowest hypervolume value in the 10 runs on DTLZ7 problem. (a) EI_e ; (b) EIm ; (c) EI_h ; (d) EIM_e ; (e) EIM_m ; (f) EIM_h .

points and 2 objectives, the Euclidean distance-based EIM criterion is more than 10 times faster than the Euclidean distance-based EI criterion. When the number of objectives and non-dominated front points increases, the computational time of the Euclidean distance-based EI criterion increases rapidly, but the computational time of the Euclidean distance-based EIM criterion increases very slowly in comparison. For example, the computational time of the 6-objective Euclidean distance-based EI criterion increases from 8.8×10^{-4} seconds to 1.5×10^1 seconds when the number of the non-dominated front points increase from 10 to 1000, but the computational time only increases from 2.0×10^{-5} seconds to 2.6×10^{-4} seconds for the Euclidean distance-based EIM criterion.

In Fig. 17, EI_h -IRS criterion is competitive to the proposed EIM_h criterion for the instance with 2 objectives and 10 non-dominated front points, the average computational time is 3.1×10^{-5} seconds to 2.8×10^{-5} seconds. However, the computational time of EI_h -IRS criterion increases rapidly with respect to the number of objectives and the number of non-dominated front points. The EI_h -WFG code is the current fastest available algorithm for the hypervolume-based EI criterion when the number of objectives is higher than three, but it is still significantly slower than the proposed EIM_h criterion.

Overall, it can be seen that the computation time increases rapidly with respect to the number of the objectives and the number of the non-dominated front points for the state-of-the-art EI criteria, but scales well with respect to the number of the objectives and the number of the non-dominated front points for the three proposed EIM criteria. The current fastest available algorithms need more than 10 seconds to calculate the EI criteria for the instance with 6 objectives and 1000 non-dominated front points, whereas the proposed EIM criteria need no more than 3×10^{-4} seconds. This means the state-of-the-art EI criteria is no longer feasible when dealing with problems with large number of objectives and large number of non-dominated front points, but the proposed EIM criteria have no computational problem to be used in these problems.

The natures of the multiobjective EI criteria and the multiobjective EIM criteria are different. The multiobjective EI criteria are calculated using $(k+1)^m$ (k is the number of non-dominated front points and m is the number of objectives) m -dimensional piecewise integrations and the multiobjective EIM criteria are calculated using $k \times m$ one-dimensional integrations. Although the computation time of the EI criteria can be reduced by using a compiled programming language, or optimized code, the ‘curse of dimensionality’ can not be avoided because of the nature of these multiobjective EI criteria.

VIII. DEALING WITH CONSTRAINTS

Most practical multiobjective optimization problems are subject to a certain number of constraints. In this paper, we assume that the constrained multiobjective problem involves q inequality constraints $g_i(\mathbf{x}) \leq 0$ (the constraint $g \geq 0$ can be easily transformed to $-g \leq 0$, and the equality constraint $g = 0$ can be transformed to two inequality constraints $g - \varepsilon \leq 0$

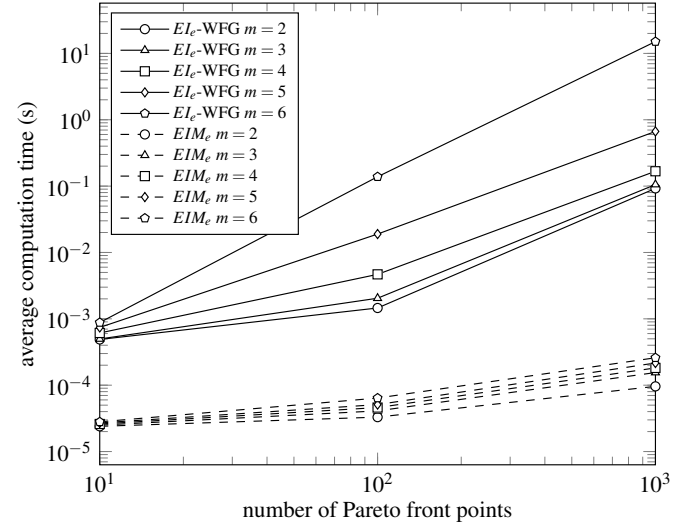


Fig. 15. The computational time (in seconds) of the Euclidean distance-based EI and EIM criteria.

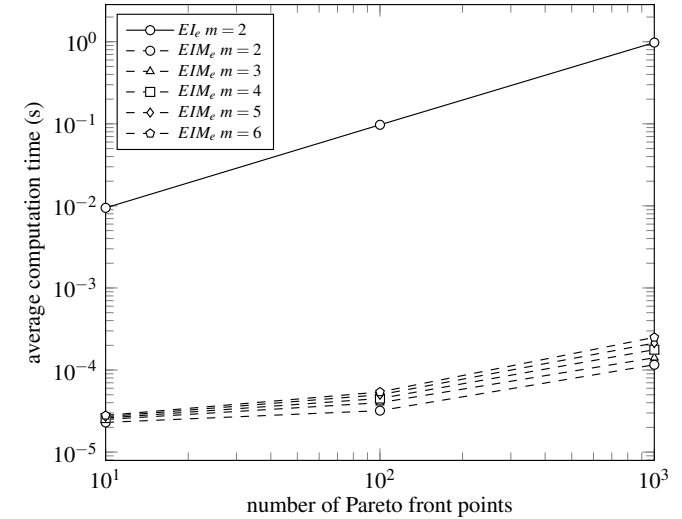


Fig. 16. The computational time (in seconds) of the maximin distance-based EI and EIM criteria.

and $-g - \varepsilon \leq 0$, where ε is a small positive constant), where $i = 1, 2, \dots, q$. Also the constraints are assumed to be black-box and expensive to calculate, thus only a few number of evaluations are allowed.

In order to solve the expensive constrained multiobjective optimization problems, we combine the probability of feasibility (PoF) [5], [12], [27] criterion with the proposed multi-objective EIM criteria. Each constraint is approximated by a Kriging model using the initial design points, the probability that the studying point satisfies the i th constraint is [12]:

$$PoF_i(\mathbf{x}) = \Phi\left(\frac{0 - \hat{g}_i(\mathbf{x})}{s_{gi}(\mathbf{x})}\right), \quad (30)$$

where $\hat{g}_i(\mathbf{x})$ and $s_{gi}(\mathbf{x})$ are the Kriging prediction and the square root mean error of the i th constraint at the studying point \mathbf{x} , and $i = 1, 2, \dots, q$. Then the probability that the

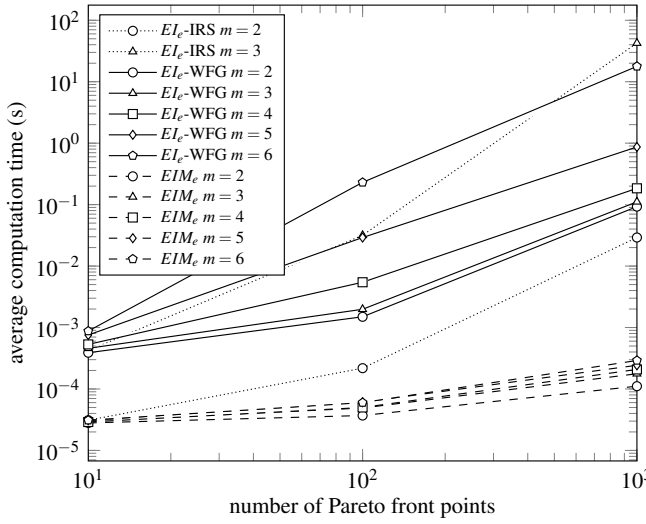


Fig. 17. The computational time (in seconds) of the hypervolume-based EI and EIM criteria.

studying point satisfies all the constraints is defined by the probability of feasibility (PoF) [12]:

$$PoF(\mathbf{x}) = \prod_{i=1}^q \left[\Phi\left(\frac{0 - \hat{g}_i(\mathbf{x})}{s_{gi}(\mathbf{x})}\right) \right]. \quad (31)$$

The value of the PoF criterion is between zero and one, and the higher the PoF value the greater probability the studying point will satisfy the constraints. Multiplying the three proposed multiobjective EIM criteria in (23) (25) and (28) by the PoF in (31) derives the corresponding constrained EIM (CEIM) criteria:

$$CEIM_e(\mathbf{x}) = \min_{j=1}^k \sqrt{\sum_{i=1}^m (EI_i^j(\mathbf{x}))^2} \times \prod_{i=1}^q \left[\Phi\left(\frac{0 - \hat{g}_i(\mathbf{x})}{s_{gi}(\mathbf{x})}\right) \right], \quad (32)$$

$$CEIM_m(\mathbf{x}) = \min_{j=1}^k \left[\max_{i=1}^m EI_i^j(\mathbf{x}) \right] \times \prod_{i=1}^q \left[\Phi\left(\frac{0 - \hat{g}_i(\mathbf{x})}{s_{gi}(\mathbf{x})}\right) \right], \quad (33)$$

and

$$CEIM_h(\mathbf{x}) = \min_{j=1}^k \left[\prod_{i=1}^m (r_i + EI_i^j(\mathbf{x}) - f_i^j) - \prod_{i=1}^m (r_i - f_i^j) \right] \times \prod_{i=1}^q \left[\Phi\left(\frac{0 - \hat{g}_i(\mathbf{x})}{s_{gi}(\mathbf{x})}\right) \right]. \quad (34)$$

The first term of the constrained EIM criterion prefers candidates that have large improvements toward the Pareto front and the second term prefers candidates that have great probability to satisfy all the constraints. By combining the two components together, the constrained EIM criteria are able to guide the search towards places that are not only near the Pareto front but also very likely to be feasible.

In order to validate the proposed constrained EIM criteria, a variant of the classic Nowacki beam problem [54] is used. This constrained multiobjective optimization problem is defined

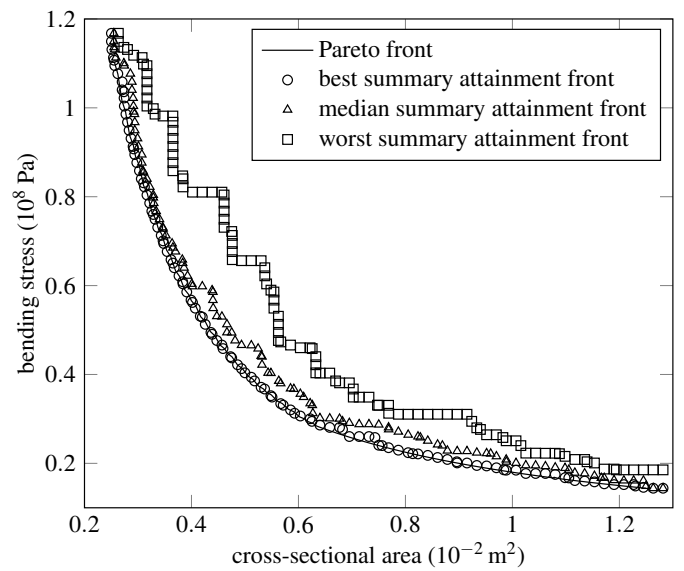


Fig. 18. The Pareto front and summary attainment surfaces of the 21 approximation fronts obtained by the $CEIM_e$ criterion of the Nowacki beam optimization problem.

in [27] and the constraints can be classified as NRSK (Non-quantifiable, Relaxable, Simulation and Known) according to the taxonomy [55]. The detail of the problem is described in Appendix B. 21 points are used for initial design and another 29 points are allowed for further iteration. For each constrained EIM criterion, the experiments are run 21 times using 21 different initial designs. The best, median and worst summary attainment surfaces [56] of the 21 Pareto approximations obtained by each criterion are shown in Figs. 18-20. The figures show that the proposed constrained EIM criteria can find well-distributed feasible solutions of the Nowacki beam optimization problem using only 50 evaluations. It turns out that the probability of feasibility criterion works fine with the proposed multiobjective EIM criteria to solve the 2-objective Nowacki beam optimization problem. More complex and higher-objective constrained problems will be investigated in further work.

IX. CONCLUSION

This paper proposes three multiobjective infill criteria for expensive multiobjective Kriging-based optimization. The proposed criteria avoid tedious piecewise multivariate integration which limits the usage of the state-of-the-art multiobjective EI criteria in problems when the number of objectives is higher than two. The proposed approach builds an EI matrix which contains all information about the single-objective EIs upon all the non-dominated front points in all directions, then uses the forms of multiobjective improvement to aggregate all the EIs into scalar metrics. The principal advantage of the proposed EIM criteria is that they are simple and closed form expressions, therefore, significantly cheaper to evaluate than the state-of-the-art EI criteria.

Test problems with number of objectives from 2 to 6 are used to investigate the efficiency of the proposed EIM criteria. The proposed EIM criteria outperform or perform similarly

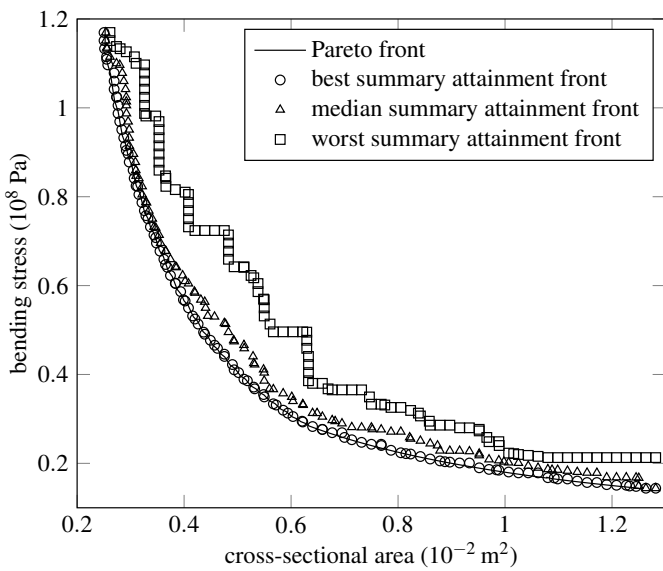


Fig. 19. The Pareto front and summary attainment surfaces of the 21 approximation fronts obtained by the $CEIM_m$ criterion of the Nowacki beam optimization problem.

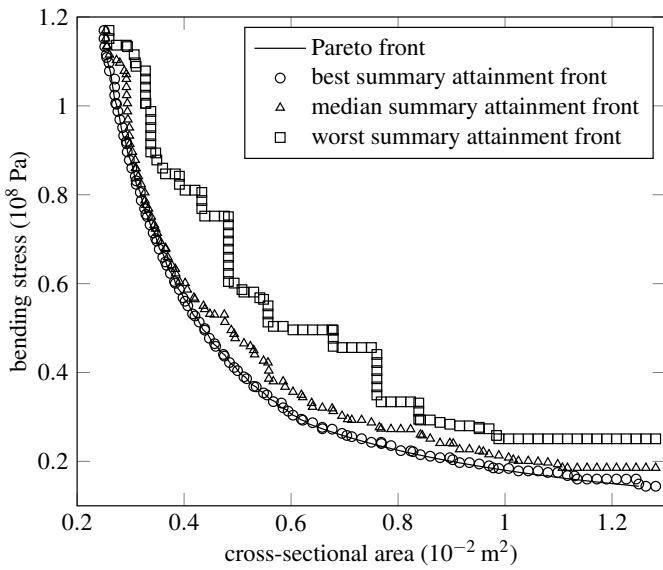


Fig. 20. The Pareto front and summary attainment surfaces of the 21 approximation fronts obtained by the $CEIM_h$ criterion of the Nowacki beam optimization problem.

to the state-of-the-art EI criteria. The proposed EIM criteria are more suitable for use in practical problems due to their high efficiency in approximating the Pareto front and low computational cost to calculate compared to the state-of-the-art. We use the probability of feasibility criterion to extend the proposed EIM criteria to deal with constraints. The results show that the proposed constrained EIM criteria are able to gain well-distributed Pareto front approximations on the Nowacki beam problem. As further research work, we would like to apply the proposed multiobjective EIM criteria to more complex test problems and real-world engineering problems.

APPENDIX A

THE MATLAB CODE OF THE THREE PROPOSED EIM CRITERIA

The MATLAB[®] code of the three proposed EIM criteria are given in the following.

```
function y=EIM_Euclidean(u,s,F)
n=size(F,1);
lamda=(F-ones(n,1)*u)./(ones(n,1)*s);
EIM=(F-ones(n,1)*u).*gausscdf(lamda)+
ones(n,1)*s.*gausspdf(lamda);
y=min(sqrt(sum(EIM.^2,2)));
end
```

```
function y=EIM_Maximin(u,s,F)
n=size(F,1);
lamda=(F-ones(n,1)*u)./(ones(n,1)*s);
EIM=(F-ones(n,1)*u).*gausscdf(lamda)+
ones(n,1)*s.*gausspdf(lamda);
y=min(max(EIM,[],2));
end
```

```
function y=EIM_Hypervolume(u,s,F,r)
n=size(F,1);
lamda=(F-ones(n,1)*u)./(ones(n,1)*s);
EIM=(F-ones(n,1)*u).*gausscdf(lamda)+
ones(n,1)*s.*gausspdf(lamda);
y=min(prod(r(ones(n,1),:)-F+EIM,2)-prod
(r(ones(n,1),:)-F,2));
end
```

In the three functions, u and s are the Kriging prediction vector and the rooted mean squared error vector of the studying point respectively; F is current non-dominated front points and r is the reference point in the hypervolume-based EIM criterion. $gausscdf$ and $gausspdf$ are the Gaussian cumulative distribution function and probability density function respectively, and are defined as following.

```
function y=gausscdf(x)
y=0.5*(1+erf(x/sqrt(2)));
end
```

```
function y=gausspdf(x)
y=1/sqrt(2*pi)*exp(-x.^2/2);
end
```

APPENDIX B

THE NOWACKI BEAM OPTIMIZATION PROBLEM

The variant of the classic Nowacki beam problem [54] is trying to design a tip-loaded encastre cantilever beam with minimum cross-sectional area A and lowest bending stress σ_B subject to a number of constraints. The length of the rectangular beam is $l = 1.5$ m, the tip-load F is 5 kN. The height h and breadth b of the beam are the two design variables.

The constrained multiobjective optimization problem can be described as following:

$$\begin{aligned} & \text{find } (h, b) \\ & \text{minimize } A, \sigma_B \\ & \text{subject to } \delta \leq 5\text{mm} \\ & \quad \sigma_B \leq \sigma_Y \\ & \quad \tau \leq \sigma_Y / 2 \\ & \quad h/b \leq 10 \\ & \quad F_{cr} \geq f \times F. \end{aligned} \quad (35)$$

In the formula, $A = h \times b$ is cross-sectional area of the beam; $\sigma_B = 6Fl/(bh^2)$ is the bending stress; $\delta = Fl/(3EI_Y)$ is the maximum tip deflection, where $E = 216.62 \text{ GPa}$ and $I_Y = bh^3/12$; $\sigma_Y = 240 \text{ MPa}$ is yield stress of the material; $\tau = 3F/(2bh)$ is the shear stress; $F_{cr} = (4/l^2)\sqrt{G_I EI_Z/(1-\nu^2)}$ is failure force of buckling, where f is a safety factor of 2, $G = 86.65 \text{ GPa}$ is the shear modulus, $\nu = 0.27$, $I_T = (b^3h + bh^3)/12$ and $I_Z = b^3h/12$.

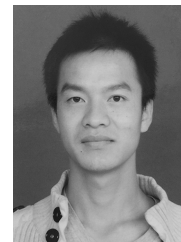
ACKNOWLEDGMENT

We would like to thank Ivo Couckuyt for kindly providing the codes of the fast calculation of the Euclidean distance-based EI criterion and hypervolume-based EI criterion.

REFERENCES

- [1] K. Deb, A. Pratap, S. Agarwal, and T. Meyarivan, "A fast and elitist multiobjective genetic algorithm: NSGA-II," *IEEE Trans. Evol. Comput.*, vol. 6, no. 2, pp. 182–197, Apr. 2002.
- [2] T. W. Simpson, A. J. Booker, D. Ghosh, A. A. Giunta, P. N. Koch, and R.-J. Yang, "Approximation methods in multidisciplinary analysis and optimization: a panel discussion," *Struct. Multidiscip. Optim.*, vol. 27, no. 5, pp. 302–313, Jul. 2004.
- [3] G. G. Wang and S. Shan, "Review of metamodeling techniques in support of engineering design optimization," *J. Mech. Des.*, vol. 129, no. 4, pp. 370–380, Apr. 2007.
- [4] F. A. C. Viana, T. W. Simpson, V. Balabanov, and V. Toropov, "Special section on multidisciplinary design optimization: Metamodeling in multidisciplinary design optimization: How far have we really come?" *AIAA Journal*, vol. 52, no. 4, pp. 670–690, Apr. 2014.
- [5] M. Schonlau, "Computer experiments and global optimization," Ph.D. dissertation, Univ. of Waterloo, 1997.
- [6] D. R. Jones, M. Schonlau, and W. J. Welch, "Efficient global optimization of expensive black-box functions," *J. Glob. Optim.*, vol. 13, no. 4, pp. 455–492, Dec. 1998.
- [7] D. R. Jones, "A taxonomy of global optimization methods based on response surfaces," *J. Glob. Optim.*, vol. 21, no. 4, pp. 345–383, Dec. 2001.
- [8] J. Mockus, V. Tiesis, and A. Zilinskas, "The application of bayesian methods for seeking the extremum," in *Towards Global Optimisation*, L. C. W. Dixon and G. P. Szegö, Eds. North-Holland Amsterdam, 1978, vol. 2, pp. 117–128.
- [9] J. Mockus, *Bayesian approach to global optimization: theory and applications*. Springer Science & Business Media, 2012, vol. 37.
- [10] W. Ponweiser, T. Wagner, and M. Vincze, "Clustered multiple generalized expected improvement: A novel infill sampling criterion for surrogate models," in *Proc. IEEE Congr. Evol. Comput.*, Hong Kong, China, Jun. 2008, pp. 3515–3522.
- [11] J. P. C. Kleijnen, W. van Beers, and I. van Nieuwenhuyse, "Expected improvement in efficient global optimization through bootstrapped kriging," *J. Glob. Optim.*, vol. 54, no. 1, pp. 59–73, Sep. 2012.
- [12] J. M. Parr, A. J. Keane, A. I. J. Forrester, and C. M. E. Holden, "Infill sampling criteria for surrogate-based optimization with constraint handling," *Eng. Optimiz.*, vol. 44, no. 10, pp. 1147–1166, Oct. 2012.
- [13] S. Koullias and D. N. Mavris, "Methodology for global optimization of computationally expensive design problems," *J. Mech. Des.*, vol. 136, no. 8, pp. 081007–1–081007–12, Jun. 2014.
- [14] A. I. J. Forrester, A. J. Keane, and N. W. Bressloff, "Design and analysis of ‘noisy’ computer experiments," *AIAA Journal*, vol. 44, no. 10, pp. 2331–2339, Oct. 2006.
- [15] D. Huang, T. T. Allen, W. I. Notz, and N. Zeng, "Global optimization of stochastic black-box systems via sequential kriging meta-models," *J. Glob. Optim.*, vol. 34, no. 3, pp. 441–466, Mar. 2006.
- [16] V. Picheny, T. Wagner, and D. Ginsbourger, "A benchmark of kriging-based infill criteria for noisy optimization," *Struct. Multidiscip. Optim.*, vol. 48, no. 3, pp. 607–626, Sep. 2013.
- [17] M. T. M. Emmerich, "Single- and multi-objective evolutionary design optimization assisted by gaussian random field metamodels," Ph.D. dissertation, Dortmund Univ., 2005.
- [18] M. T. M. Emmerich, K. C. Giannakoglou, and B. Naujoks, "Single- and multiobjective evolutionary optimization assisted by gaussian random field metamodels," *IEEE Trans. Evol. Comput.*, vol. 10, no. 4, pp. 421–439, Aug. 2006.
- [19] J. Shinkyu and S. Obayashi, "Efficient global optimization (EGO) for multi-objective problems and data mining," in *Proc. IEEE Congr. Evol. Comput.*, Sep. 2005, pp. 2138–2145.
- [20] J. Knowles, "ParEGO: A hybrid algorithm with on-line landscape approximation for expensive multiobjective optimization problems," *IEEE Trans. Evol. Comput.*, vol. 10, no. 1, pp. 50–66, Feb. 2006.
- [21] Q. Zhang, W. Liu, E. Tsang, and B. Virginas, "Expensive multiobjective optimization by MOEA/D with gaussian process model," *IEEE Trans. Evol. Comput.*, vol. 14, no. 3, pp. 456–474, Jun. 2010.
- [22] T. Wagner, M. Emmerich, A. Deutz, and W. Ponweiser, "On expected-improvement criteria for model-based multi-objective optimization," in *Parallel Problem Solving from Nature, PPSN XI*, ser. Lecture Notes in Computer Science, R. Schaefer et al., Eds. Springer Berlin Heidelberg, 2010, vol. 6238, pp. 718–727.
- [23] Ł. Łaniewski-Wołk, S. Obayashi, and S. Jeong, "Development of expected improvement for multi-objective problem," in *Proceedings of 42nd Fluid Dynamics Conference/Aerospace Numerical Simulation Symposium*, 2010.
- [24] K. Shimoyama, K. Sato, S. Jeong, , and S. Obayashi, "Comparison of the criteria for updating kriging response surface models in multi-objective optimization," in *Proc. IEEE Congr. Evol. Comput.*, Brisbane, Australia, Jun. 2012.
- [25] A. J. Keane, "Statistical improvement criteria for use in multiobjective design optimization," *AIAA Journal*, vol. 44, no. 4, pp. 879–891, Apr. 2006.
- [26] D. C. Bautista, "A sequential design for approximating the pareto front using the expected pareto improvement function," Ph.D. dissertation, The Ohio State Univ., 2009.
- [27] A. I. J. Forrester, A. Sobester, and A. J. Keane, *Engineering design via surrogate modelling: a practical guide*. John Wiley & Sons, 2008.
- [28] J. D. Svenson, "Computer experiments: Multiobjective optimization and sensitivity analysis," Ph.D. dissertation, The Ohio State Univ., 2011.
- [29] J. Svenson and T. Santner, "Multiobjective optimization of expensive-to-evaluate deterministic computer simulator models," *Comput. Stat. Data Anal.*, vol. 94, pp. 250–264, Feb. 2016.
- [30] I. Couckuyt, D. Deschrijver, and T. Dhaene, "Fast calculation of multi-objective probability of improvement and expected improvement criteria for pareto optimization," *J. Glob. Optim.*, vol. 60, no. 3, pp. 575–594, Nov. 2014.
- [31] I. Hupkens, A. Deutz, K. Yang, and M. Emmerich, "Faster exact algorithms for computing expected hypervolume improvement," in *Evolutionary Multi-Criterion Optimization*, ser. Lecture Notes in Computer Science, A. Gaspar-Cunha et al., Eds. Springer International Publishing, 2015, vol. 9019, pp. 65–79.
- [32] C. K. Williams and C. E. Rasmussen, *Gaussian processes for machine learning*. The MIT Press, 2006.
- [33] J. Sacks, W. J. Welch, T. J. Mitchell, and H. P. Wynn, "Design and analysis of computer experiments," *Statist. Sci.*, vol. 4, no. 4, pp. 409–423, Nov. 1989.
- [34] R. Balling, "The maximin fitness function: multi-objective city and regional planning," in *Evolutionary Multi-Criterion Optimization*, ser. Lecture Notes in Computer Science, C. M. Fonseca et al., Eds. Springer Berlin Heidelberg, 2003, vol. 2632, pp. 1–15.
- [35] E. Zitzler, "Evolutionary algorithms for multiobjective optimization: Methods and applications," Ph.D. dissertation, Univ. of Zurich, 1999.
- [36] E. Zitzler, L. Thiele, M. Laumanns, C. M. Fonseca, , and V. G. da Fonseca, "Performance assessment of multiobjective optimizers: An analysis and review," *IEEE Trans. Evol. Comput.*, vol. 7, no. 2, pp. 117–132, Apr. 2003.

- [37] J. Knowles and D. Corne, "Properties of an adaptive archiving algorithm for storing nondominated vectors," *IEEE Trans. Evol. Comput.*, vol. 7, no. 2, pp. 100–116, Apr. 2003.
- [38] M. Basseur and E. K. Burke, "Indicator-based multi-objective local search," in *Proc. IEEE Congr. Evol. Comput.*, Singapore, Sep. 2007, pp. 3100–3107.
- [39] J. Bader and E. Zitzler, "HypE: An algorithm for fast hypervolume-based many-objective optimization," *Evol. Comput.*, vol. 19, no. 1, pp. 45–76, Mar. 2011.
- [40] C. M. Fonseca, L. Paquete, and M. Lopez-Ibanez, "An improved dimension-sweep algorithm for the hypervolume indicator," in *Proc. IEEE Congr. Evol. Comput.*, Jul. 2006, pp. 1157–1163.
- [41] L. While, P. Hingston, L. Barone, and S. Huband, "A faster algorithm for calculating hypervolume," *IEEE Trans. Evol. Comput.*, vol. 10, no. 1, pp. 29–38, Feb. 2006.
- [42] N. Beume, C. M. Fonseca, M. Lopez-Ibanez, L. Paquete, and J. Vahrenhold, "On the complexity of computing the hypervolume indicator," *IEEE Trans. Evol. Comput.*, vol. 13, no. 5, pp. 1075–1082, Oct. 2009.
- [43] L. While, L. Bradstreet, and L. Barone, "A fast way of calculating exact hypervolumes," *IEEE Trans. Evol. Comput.*, vol. 16, no. 1, pp. 86–95, Feb. 2012.
- [44] M. T. M. Emmerich, A. H. Deutz, and J. W. Klinkenberg, "Hypervolume-based expected improvement: Monotonicity properties and exact computation," in *Proc. IEEE Congr. Evol. Comput.*, New Orleans, LA, Jun. 2011, pp. 2147–2154.
- [45] A. Törn and A. Žilinskas, *Global optimization*, ser. Lecture Notes in Computer Science. Springer Berlin Heidelberg, 1989, vol. 350.
- [46] E. Zitzler, K. Deb, and L. Thiele, "Comparison of multiobjective evolutionary algorithms: Empirical results," *IEEE Trans. Evol. Comput.*, vol. 8, no. 2, pp. 173–195, Jun. 2000.
- [47] K. Deb, L. Thiele, M. Laumanns, and E. Zitzler, "Scalable test problems for evolutionary multi-objective optimization," Computer Engineering and Networks Laboratory (TIK), ETH Zürich, Tech. Rep. TIK Report No. 112, Jul. 2001.
- [48] S. N. Lophaven, H. B. Nielsen, and J. Søndergaard. (2002, Aug.) Dace - a matlab kriging toolbox, version 2.0. [Online]. Available: <http://www2.imm.dtu.dk/projects/dace/>
- [49] D. Gorissen, I. Couckuyt, P. Demeester, T. Dhaene, and K. Crombecq, "A surrogate modeling and adaptive sampling toolbox for computer based design," *J. Mach. Learn. Res.*, vol. 11, pp. 2051–2055, Jul. 2010.
- [50] K. Price, R. Storn, and J. Lampinen, *Differential Evolution: A practical approach to global optimization*. Springer Berlin Heidelberg, 2005.
- [51] F. Viana. (2011) Surrogates toolbox users guide, version 3.0. [Online]. Available: <http://sites.google.com/site/felipeviana/surrogatestoolbox>
- [52] C. A. C. Coello and M. R. Sierra, "A study of the parallelization of a coevolutionary multi-objective evolutionary algorithm," in *MICAI 2004: Advances in Artificial Intelligence*, ser. Lecture Notes in Computer Science, R. Monroy *et al.*, Eds. Springer Berlin Heidelberg, 2004, vol. 2972, pp. 688–697.
- [53] M. T. M. Emmerich and C. M. Fonseca, "Computing hypervolume contributions in low dimensions: Asymptotically optimal algorithm and complexity results," in *Evolutionary Multi-Criterion Optimization*, ser. Lecture Notes in Computer Science, R. H. C. Takahashi *et al.*, Eds. Springer Berlin Heidelberg, 2011, vol. 6576, pp. 121–135.
- [54] H. Nowacki, "Modelling of design decisions for cad," in *Computer Aided Design Modelling, Systems Engineering, CAD-Systems*, ser. Lecture Notes in Computer Science, J. Encarnacao, Ed. Springer Berlin Heidelberg, 1980, vol. 89, pp. 177–223.
- [55] S. L. Digabel and S. M. Wild, "A taxonomy of constraints in simulation-based optimization," *arXiv preprint arXiv:1505.07881*, 2015.
- [56] J. Knowles, "A summary-attainment-surface plotting method for visualizing the performance of stochastic multiobjective optimizers," in *International Conference on Intelligent Systems Design and Applications*, Sep. 2005, pp. 552–557.



Dawei Zhan was born in Honghu, Hubei, China in 1989. He received the B.S. degree in naval architecture and ocean engineering from Huazhong University of Science and Technology, Wuhan, China, in 2012. He is currently working toward the Ph.D. degree with the naval architecture and ocean engineering, Huazhong University of Science and Technology.

His research interests include surrogate modelling and surrogate-based single-objective and multiobjective optimization.



Yuansheng Cheng was born in Wuhan, Hubei, China in 1962. He received the B.S. and M.S. degree in naval architecture and ocean engineering from Huazhong University of Science and Technology, Wuhan, China in 1987 and the Ph.D. degree in structural engineering from The University of Hong Kong, Hong Kong, China in 2000.

He is currently a Professor in the School of Naval Architecture and Ocean Engineering, Huazhong University of Science and Technology. His research interests include structural mechanics, structural impact dynamics, multidisciplinary optimization and multiobjective optimization.



Jun Liu was born in Suizhou, Hubei, China in 1981. He received the B.S. and Ph.D. degree in naval architecture and ocean engineering from Huazhong University of Science and Technology, Wuhan, China in 2004 and 2009 respectively.

He is currently a Associate Professor in the School of Naval Architecture and Ocean Engineering, Huazhong University of Science and Technology. His research interests include structural impact dynamics, structural vibration and noise control and structural optimization.